

2014 Mobile Communications and Infrastructure



A Special Supplement to

**Microwave
Journal**



Broad Product Portfolio Supporting All Mobile Platforms



For more information please visit www.skyworksinc.com.



Join our customer email program instantly by scanning the QR code with your smartphone, or visit our Web site at www.skyworksinc.com.

***Visit Us at GSMA Mobile World Congress 2015 • Hall 6, Stand 6C41
Barcelona, Spain • March 2-5***

USA: 781-376-3000 • Asia: 886-2-2735 0399 • Europe: 33 (0)1 43548540 • Email: sales@skyworksinc.com

www.skyworksinc.com • NASDAQ: SWKS • [in](#) [f](#) [t](#)



Contents

Cover Feature

4 Small Wavelengths - Big Potential: Millimeter Wave Propagation Measurements for 5G

Sijia Deng, Christopher J. Slezak, George R. MacCartney Jr., Theodore S. Rappaport, NYU WIRELESS, NYU Polytechnic School of Engineering

Technical Features

14 Understanding Envelope Tracking and Its Measurement Challenges

Yu Qian, Keysight Technologies

18 Six LTE Receiver Measurements Every Wireless Engineer Should Know

David A. Hall, National Instruments

22 Design of an 8x8 MIMO Broadband RF Subsystem for Future WLAN

Li Zhao, Jian-Yi Zhou, Wen-Wen Yang, Zhi-Qiang Yu and Li-Na Cao, Southeast University

28 Smart Antennas and Front End Modules in Q-Band for Backhaul Networks

R. Vilar, J. Marti, Universitat Politècnica de Valencia; R. Czarny, Thales Research and Technology; M. Sypek, M. Makowski, Ortech SP. Z O.O.; C. Martel, T. Crépin, F. Boust, Office National d'Etudes et de Recherches Aérospatiales; R. Joseph, K. Herbertz, T. Bertuch, Fraunhofer Institute for High Frequency Physics and Radar Techniques FHR; A. LeFevre, Thales Communications & Security SA; F. Magne, Bluwan Ltd.

Special Report

36 Disruptive Factors in the Global Long Haul Market

Emmy Johnson, Sky Light Research

Product Features

40 Locating Sources of Interference

Cyril Noger, Anritsu S.A.

44 Transcorder Records 80 MHz Bandwidth Between 50 MHz and 6 GHz

QRC Technologies

Tech Briefs

46 Field Analyzer with PIM Testing Capability

Anritsu Co.

46 Low PIM, Plenum Rated Cable Assembly and Mini-DIN Connector

Times Microwave

48 DC to 6 GHz SDR

Per Vices

Company Showcase

49 Company profiles highlighting mobile communications infrastructure and new products



AUGMENTED REALITY: HOW IT WORKS

STEP 1

Download the free Layar app from the iTunes (iOS) or Google Play (Android) store.

STEP 2

Launch the app to view enhanced content on any page with the **layar** logo.

STEP 3

Frame the entire page in the screen and tap to experience enhancements (tap screen again for full screen view).

Refer to page 50 for this month's participants
AR pages may expire after 60 days

STAFF

PUBLISHER: CARL SHEFFRES

EDITOR: PATRICK HINDLE

TECHNICAL EDITOR: GARY LERUDE

MANAGING EDITOR: JENNIFER DiMARCO

ASSOCIATE TECHNICAL EDITOR: CLIFF DRUBIN

MULTIMEDIA STAFF EDITORS:

BARBARA WALSH AND LESLIE NIKOU

CONSULTING EDITOR: HARLAN HOWE, JR.

CONSULTING EDITOR: FRANK BASHORE

CONSULTING EDITOR: RAYMOND PENGELLY

CLIENT SERVICES MANAGER:

KRISTEN ANDERSON

WEB EDITOR: CHRIS STANFA

AUDIENCE DEVELOPMENT MANAGER:

CAROL SPACH

TRAFFIC MANAGER: EDWARD KIESSLING

DIRECTOR OF PRODUCTION & DISTRIBUTION:

ROBERT BASS

ART DIRECTOR: JANICE LEVENSON

GRAPHIC DESIGNER: SACHIKO STIGLITZ

EUROPE

INTERNATIONAL EDITOR: RICHARD MUMFORD

OFFICE MANAGER: NINA PLESU

CORPORATE STAFF

CEO: WILLIAM M. BAZZY

PRESIDENT: IVAR BAZZY

VICE PRESIDENT: JARED BAZZY



Scan page
using **layar** app

Small Wavelengths – Big Potential: Millimeter Wave Propagation Measurements for 5G

Sijia Deng, Christopher J. Slezak, George R. MacCartney Jr. and
Theodore S. Rappaport
NYU WIRELESS, NYU Polytechnic School of Engineering, Brooklyn, N.Y.

This article introduces wideband millimeter wave propagation measurements and the sliding correlator channel sounder system used to measure millimeter wave channels in New York City. The measurement system includes a 400 to 750 Megachips-per-second sliding correlator channel sounder that utilizes steerable directional horn antennas at both the transmitter and receiver. Several recent propagation measurement campaigns were conducted by the NYU WIRELESS research center in indoor and outdoor environments at the 28 and 73 GHz millimeter wave bands, resulting in directional and omnidirectional path loss models and multipath spread characteristics that are presented here. Measurement results for directional path loss, omnidirectional path loss and RMS delay spread are presented here. These results will help engineers design future millimeter wave wireless communications systems and will assist in the standardization of millimeter wave wireless networks.

As the wireless industry prepares for the impending fifth-generation (5G) wireless technology to meet the projected $1,000 \times$ growth in user demand in the coming decade, there is a need for accurate and comprehensive channel models at millimeter wave frequencies.^{1,2,4,5} Unlike previous generations of cellular technology, 5G will likely make use of the millimeter wave spectrum while also using existing UHF/microwave frequencies.

Millimeter wave frequencies (30 to 300 GHz) show great promise for the future of wireless communications because of the large raw available, unused bandwidth. In particular, over 14 GHz of available spectrum exists in the 28, 38/39, and 73 GHz bands, making

these bands excellent candidates for new mobile spectrum that will increase capacity by several orders of magnitude over today's cellular and Wi-Fi allocations.^{2,5} Recent advances in integrated circuit and antenna technology have made it possible to inexpensively and reliably manufacture wireless devices that operate at millimeter wave frequencies.^{1,4,15,32}

Millimeter wave frequencies have not been widely used for personal communications to date because of a lack of available electronic components and a common belief that rain and atmospheric attenuation are too high for mobile access communications at these high frequencies. However, in reality the additional attenuation at millimeter wave frequencies will be negligible for coverage distances on the

order of several hundred meters.⁵⁻⁷ Urban cellular deployments already use smaller cell sizes to meet growing capacity demands, thus millimeter wave cells will have similar density to deployments in use in today's urban areas.⁶

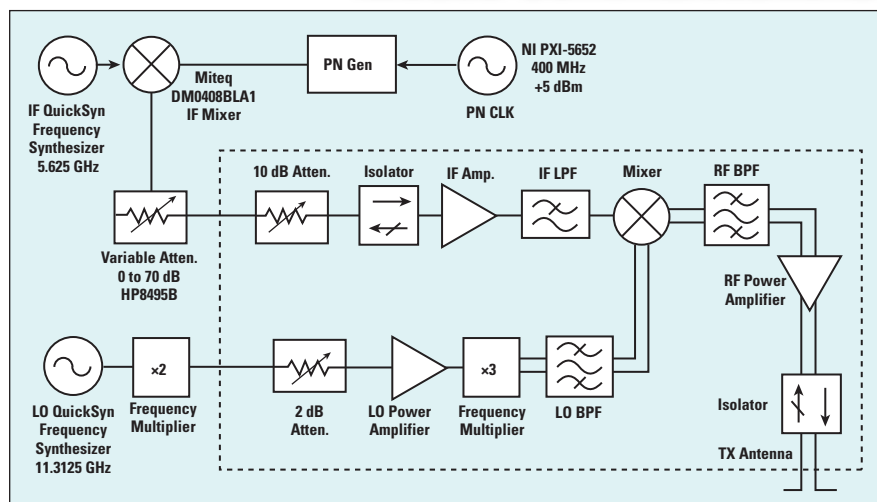
The uncharted millimeter wave spectrum requires carefully planned measurements in order to develop channel models to support equipment design and the standardization process of the air interface. Since 2012, the NYU WIRELESS research center has performed measurements at 28 and 73 GHz in New York City. These measurements have been used to develop channel models that are being used by researchers throughout industry and academia.^{4-14,27,28} Earlier measurements in Austin, Texas during the summer of 2011 explored the 38 and 60 GHz bands, using a 400 and 750 Megachips-per-second (Mcps) spread spectrum binary phase shift keying (BPSK) channel sounder, very similar to the channel sounder used for the New York City measurements.^{20,26,29,30,31}

MEASUREMENT APPROACH AND TEST SYSTEM

To conduct wideband millimeter wave channel measurements with angle of arrival and departure information, as well as high resolution multipath and received power, NYU WIRELESS makes use of a custom-built BPSK sliding correlator channel sounder. Unlike systems using vector network analyzers, there is no need for phasing cables between the transmitter (Tx) and receiver (Rx). Without the need for connecting the Tx and Rx, separation distances can be measured up to hundreds of meters in non-line-of-sight (NLOS) conditions. The system triggers from the strongest arriving multipath energy and is being upgraded with GPS-controlled cesium-standard clocks for absolute timing measurements.

The use of sliding correlation allows the channel sounder to measure over very large bandwidths.^{3,25} Transmission begins with the generation of a baseband pseudorandom noise (PN) signal. The PN sequence is created by an 11-bit linear feedback shift register (LFSR), yielding a PN sequence with a length of $2^{11}-1 = 2047$.

At the receiver, the signal is de-



▲ Fig. 1 Block diagram of the transmitter used to characterize the 73 GHz channel.

modulated into its baseband in-phase (I) and quadrature (Q) components. These signals are then cross-correlated with a PN sequence identical to the Tx. The PN sequence at the Rx, however, is generated at a chip rate slightly offset from the Tx chip rate. For the outdoor New York City measurements, the Tx transmits at 400 Mcps and the Rx chip rate is 399.95 Mcps. The offset in chip rates gives rise to the slide factor, γ , which is calculated as:

$$\gamma = \frac{f_c}{f_c - f'_c}$$

where f_c and f'_c are the Tx and Rx chip rates, respectively.^{3,16}

Due to the autocorrelation properties of PN sequences, the cross-correlation will be orders of magnitude larger when the two sequences are aligned than when not. These correlations can be performed separately but concurrently for the I and Q components, yielding two signals $I(\tau)$ and $Q(\tau)$.¹⁷ The correlation peaks that occur when the sequences are aligned can be sampled and used to recover the channel's power delay profile (PDP) $p(\tau)$.

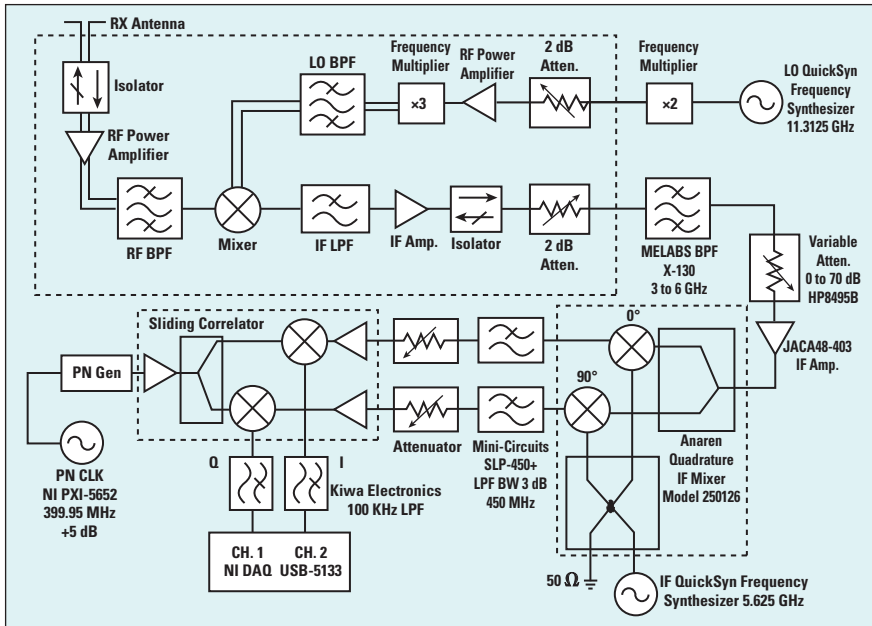
$$p(\tau) = I^2(\tau) + Q^2(\tau)$$

One of the most important features of the sliding correlator is the time dilation it provides. The sliding correlator has the effect of compressing the PDP's bandwidth drastically, equivalent to the original Tx chip rate divided by the slide factor.^{3,18} For chip rates of 400 Mcps at the Tx and 399.95 Mcps at the Rx, the signals $I(\tau)$ and $Q(\tau)$ will each have a bandwidth of only 50 kHz.

Although the sliding correlation process approximates the autocorrelation of a PN sequence, there is still improvement to be made after the time-dilated PDP has been recovered. The compression to a very narrow bandwidth offers the opportunity to lowpass filter the signal and reject a considerable amount of distortion that is present at higher frequencies.¹⁶ Once this signal has been filtered, the true un-dilated PDP can be recovered.

There are several parameters that influence the performance of a sliding correlator, but the dynamic range in particular is often the greatest concern when considering channel sounder performance.¹⁹ The theoretical dynamic range is determined from the length of the PN sequence, and is 66.2 dB for a sequence of length 2047.¹⁹

Figure 1 shows the block diagram of the transmitter system for the 73 GHz measurements. The channel sounding system uses QuickSyn signal generators provided by National Instruments (NI) for an intermediate frequency (IF) at 6.625 GHz. The 400 Mcps baseband PN sequence, produced by a PN sequence generator, is first mixed with the 5.625 GHz IF to obtain the second stage IF spread spectrum signal. The 22.625 GHz LO frequency is tripled by a frequency multiplier to 67.875 GHz, which drives the mixing operation with the spread spectrum IF signal. This generates a spread spectrum RF signal centered at 73.5 GHz with an 800 MHz first null-to-null RF bandwidth.¹⁰



▲ Fig. 2 Block diagram of the receiver used to characterize the 73 GHz channel.

TABLE 1 SPECIFICATIONS FOR THE 28 AND 73 GHz CHANNEL SOUNDERS		
Carrier Frequency	28 GHz	73.5 GHz
Chip Sequence Length	$2^{11} - 1 = 2047$	
Chip Sequence Clock Rate (Tx)	400 MHz	
Chip Sequence Clock Rate (Rx)	399.95 MHz	
First Null-to-Null RF Bandwidth	800 MHz	
Slide Factor	8000	
Tx Antenna Gain	24.5 dBi / 15 dBi	27 dBi / 20 dBi
Tx Antenna AZ HPBW	10.9°/30°	7°/ 15°
Tx Antenna EL HPBW	8.6°/30°	7°/ 15°
Rx Antenna Gain	24.5 dBi / 15 dBi	27 dBi / 20 dBi
Rx Antenna AZ HPBW	10.9°/ 30°	7°/15°
Rx Antenna EL HPBW	8.6°/ 30°	7°/15°
Antenna Polarization	VV	VV/VH
Maximum Tx Power	30 dBm	14.6 dBm
Maximum Measurable Path Loss	178 dB	181 dB



▲ Fig. 3 28 GHz measurement sites near NYU's Manhattan campus.

28 GHz are very similar to those shown for 73 GHz in Figures 1 and 2.

Directional horn antennas with various directive gains are used to provide spatial discrimination similar to what will be used in future millimeter wave systems.^{1,15,32} By using directional antennas that can be rotated in the azimuth and elevation planes, angle of arrival (AOA) and angle of departure (AOD) information can be obtained by taking measurements across different AOA and AOD combinations.

Table 1 summarizes the specific parameters of the channel sounders used for each measurement campaign. AZ denotes azimuth, EL is elevation and HPBW is half-power beamwidth. VV indicates that the Tx and Rx horn antennas are both vertically polarized; VH denotes that the Tx antenna is vertically polarized and that the Rx antenna is horizontally polarized.

OUTDOOR MEASUREMENT CAMPAIGNS

The 28 GHz outdoor propagation measurements were conducted at three transmit locations and 25 receive locations in downtown Manhattan,⁸ shown in **Figure 3**. The three transmit locations are depicted with yellow stars, and the receive locations with green circles and purple squares. The green circles represent visible receive sites, and the purple squares depict receive locations blocked by obstructions in this view.

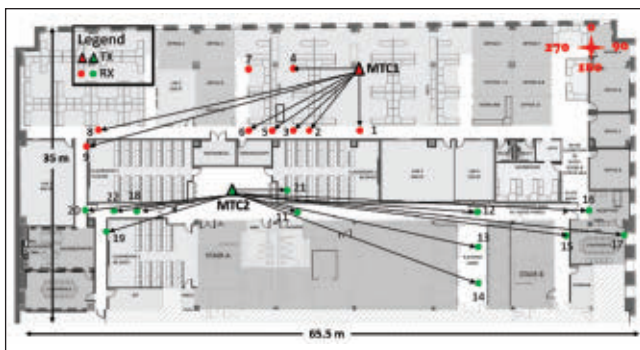
The 75 total Tx-Rx combinations comprised of Tx-Rx separation distances from 19 to 425 m. The channel sounder employed a 24.5 dBi gain antenna (10° HPBW) at the Tx, and either a 15 dBi (30° HPBW) or 24.5 dBi gain antenna (10° HPBW) at the Rx. The measurements were performed for a base station-to-mobile scenario, with Rx antennas at a mobile height of 1.5 m. Tx antennas were placed on relatively low rooftops, with two Tx locations 7 m above ground level (AGL) and one Tx location 17 m AGL. For each Tx-Rx location combination, 10 sets of measurements were conducted for various Tx and Rx azimuth and elevation angle configurations.

In addition to the Manhattan measurements, 28 GHz outdoor propagation measurements were also performed in downtown Brooklyn. These measurements were conducted for

Figure 2 shows the block diagram of the receiver system for 73 GHz measurements. The received signal is down-converted from the 73.5 GHz RF to the 5.625 GHz IF. The LO frequency at 22.625 GHz is the same as on the Tx side. The sliding process correlates the 399.95 Mcps baseband signal generated by the Rx PN sequence generator and the baseband equivalent received I and Q signals from the down-converter, resulting in a time-dilated autocorrelation with a bandwidth of 50 kHz. The NI DAQ digitizer samples the time-dilated pulse on both the I and Q channels at 2 Mega-samples-per-second (Msps). The Tx and Rx channel sounder block diagrams for



▲ Fig. 4 73 GHz measurement sites around NYU's Manhattan campus.



▲ Fig. 5 Locations for the 73 GHz indoor measurements²²

one Tx and 11 Rx locations, with the Tx-Rx separation distance ranging from 75 to 125 m. At three locations, the Rx was moved in half-wavelength increments on an automated 10-wave-length long linear track. This configuration studied small-scale fading, which impacts MIMO performance.²³

The 73 GHz outdoor propagation measurements were conducted in downtown Manhattan, at five transmit and 27 receive locations, as shown in **Figure 4**. The five transmit locations are denoted by yellow stars. Two were on the two-story rooftop of the Coles Recreational Center (7 m high), two on the second floor balcony of the Kimmel Center (7 m high), and one on the fifth-story balcony of the Kaufman building of the Stern Business School (17 m high). Tx-Rx separation distances

es ranged from 30 to 216 m.

A total of 36 unique mobile access and 38 backhaul link combinations were measured. Rx antennas at heights of 2 and 4.06 m were used to emulate base station-to-mobile links and wireless backhaul links, respectively. For each Tx-Rx combination, up to 12 measurement sweeps were conducted to generate omnidirectional path loss models.¹²

INDOOR MEASUREMENT CAMPAIGN

An extensive indoor propagation measurement campaign at 73 GHz was conducted for different antenna polarizations to model a typical office environment. To measure the co- and cross-polarized channel characteristics, a pair of 20 dBi (15° HPBW) antennas was used. Two transmit and 21 receive locations, shown in **Figure 5**,

were chosen to investigate the complex indoor propagation channels.

The Tx-Rx separation distance ranged from 6 to 46 m. The Tx antenna was set at a height of 2.5 m near the ceiling to imitate current indoor wireless access points; the Rx was set at a height of 1.5 m (similar to the height of a mobile phone carried by a person). For each Tx and Rx location combination, eight measurements with various AOD and AOA and co- and cross-polarization combinations were measured.²¹

MEASUREMENT RESULTS

Measurement results from the 28 and 73 GHz outdoor and 73 GHz indoor campaigns include directional path loss models, omnidirectional path loss models and direction root

mean square (RMS) delay spread characteristics.

Directional path loss values were obtained from individual unique pointing angles for all measurements. Directional path loss models are important, since 5G systems will use narrow beam directional antennas and will take advantage of beamforming and beam combining technologies.

Close-in free space reference distance path loss at a reference distance d_0 is expressed by the following equation:

$$PL(d)[dB] = PL(d_0) + 10\bar{n} \log_{10} \left(\frac{d}{d_0} \right) + X_\sigma \quad (1)$$

where \bar{n} is the best fit minimum mean square error (MMSE) path loss exponent (PLE), and X_σ is a zero mean Gaussian random variable with a standard deviation σ in dB, also known as the shadowing factor, caused by large-scale random variations in the channel.³ The PLE is introduced to describe the propagation attenuation caused by the channel.

Figure 6 shows outdoor directional path loss models using a 1 m close-in free space reference distance for 28 and 73 GHz. Red crosses represent the NLOS path loss value measurements, blue triangles represent the best path loss values for a specific Tx-Rx location combination and green circles represent line-of-sight (LOS) path loss. Path loss models are simplified using a d_0 of 1 m, as it removes the denominator term seen in Equation 1.

For LOS scenarios, the PLE in outdoor and indoor environments for both 28 and 73 GHz is favorable, close to the theoretical free space path loss (FSPL) of $n = 2$.

The NLOS measurements also include measurements at LOS environment when the TX and RX antennas are not directly on boresight with each other. For NLOS scenarios, **Figure 6a** shows a PLE of 4.5 for all locations in 28 GHz outdoor measurements with 24.5 dBi narrow beam co-polarized antennas. **Figure 6b** shows a PLE of 4.7 for 73 GHz outdoor measurements, and **Figure 6c** shows a PLE of 5.1 for 73 GHz indoor measurements with co-polarized antennas.

NLOS-best denotes the lowest path loss observed at a unique point-

ing angle for the directional NLOS channel for each Tx-Rx location combination. Figure 6 shows that the NLOS-best PLE is 3.7 for 28 GHz outdoor and that the NLOS-best PLE is 3.6 and 3.3 for 73 GHz outdoor and indoor mea-

surements, respectively. This improvement in PLE when considering the best NLOS angles is significant and shows the advantage of using beam searching and directional antennas at millimeter wave frequencies. The NLOS path loss experienced large attenuation per decade; however, the use of multiple antenna elements and beamforming and beam combining technologies can significantly decrease the path loss when considering the best possible paths.

The results show that beam combining can significantly reduce the propagation PLE³². PLE for certain Tx and Rx combinations reduces from 4.7 to 3.6 for 73 GHz outdoor scenarios using a 1 m free space reference distance. By coherently combining the four strongest signals from four distinct beams, compared to an arbitrarily pointed single beam, 28 dB of link improvement is achieved, and 10 dB of improvement when compared to a single optimum beam over a 100 m Tx-Rx separation at 73 GHz. For the 28 GHz outdoor measurements, the maximum possible improvement reaches 24 dB. The cross polarization measurements also show the potential for antenna polarization diversity systems in indoor millimeter wave communications systems.²¹

OMNIDIRECTIONAL PATH LOSS

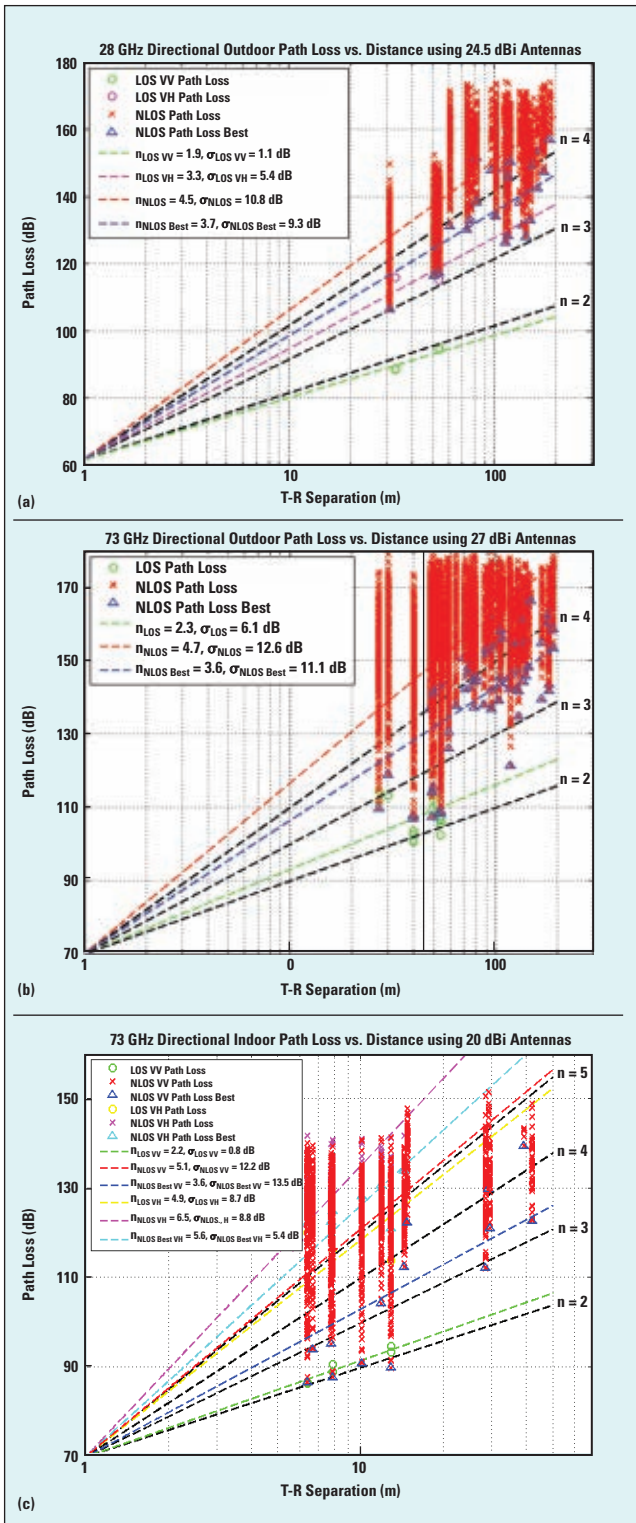
Omnidirectional path loss models are important, since they allow an arbitrary antenna pattern to be used in simulation or analysis. The existing 3GPP WINNER II and other 3GPP-like models are omnidirectional for this reason. To create omnidirectional models for each Tx-Rx location combination, the received powers at every unique azimuth and elevation angle combination were summed after removing antenna gains. This yields an omnidirectional received power for each Tx-Rx location combination, used to compute an omnidirectional path loss model.^{6,14,21}

Figure 7a shows the omnidirectional path loss models for 28 GHz outdoor LOS and NLOS measurements using a 1 m close-in reference distance. The LOS PLE of 2.3 is very close to the theoretical FSPL and has a small shadowing factor of 2.6 dB. The NLOS PLE is 3.4 with a standard deviation of 9.7 dB.¹⁴ **Figure 7b** shows the omnidirectional path loss models for 73 GHz outdoor LOS and NLOS measurements, combining the access and backhaul scenarios. The LOS PLE and NLOS PLE are similar to the 28 GHz outdoor measurements. **Figure 7c** shows the omnidirectional path model for the 73 GHz indoor measurements. The LOS PLE for VV polarization is 1.5 with shadowing factor of 0.8 dB. The corresponding LOS PLE and shadowing factor for the cross-polarized antenna are 4.5 and 6.6 dB, respectively. The NLOS omnidirectional PLE and shadowing factor for co- and cross-polarized antenna are 3.1 and 8.9 dB; and 5.3 and 0.69 dB, respectively.

The indoor omnidirectional co-polarized path loss results are very promising for an indoor environment, as the LOS PLE is lower than true free space, due to ground bounces and constructive interference from reflections. The NLOS PLE of 3.1 is also reasonable for an indoor wireless network.²¹

RMS DELAY SPREAD

RMS delay spread is one of the most important characteristics of a radio propagation channel, as it describes



▲ Fig. 6 28 GHz and 73 GHz close-in free space reference distance directional path loss in the outdoor urban environment of New York City, and indoor path loss models. 28 GHz outdoor directional path loss models (a). 73 GHz outdoor directional path loss models, considering access and backhaul Rx heights (b). 73 GHz indoor directional path loss models with VV and VH antenna polarization (c).



Low Frequency Power Combiners

MECA introduces Low Frequency addition to the H-Series, 100-watt Wilkinson high power combiner/dividers. Available in 2 & 4-way configurations covering 5 to 500 MHz. VSWR of 1.30:1 accommodating load VSWR's of 2.0:1 or better! N and SMA connectors. Weatherproof IP 67 rated.



Low PIM Compact 50 & 100 Watt Terminations

Industry leading PIM performance of -160 & -165 dBc (Typ) and covering the 698 - 2700 MHz frequency bands available in Type-N, 7/16 DIN, and 4.1/9.5 Mini-DIN, all in a compact package. Ideal for IDAS / ODAS, In-Building, base station, wireless infrastructure, 4G, and AWS applications.



Low PIM Couplers

MECA's Low PIM (-160 dBc Typ) Directional Couplers for DAS Applications feature unique air-line construction that provides for the lowest possible insertion loss, high directivity and VSWR across the 0.698-2.700 GHz bands. Rated for 500 watts average power. Nominal coupling values of 15, 20, 30 & 40 dB.

Low PIM Reactive Splitters

MECA's Low PIM (-160dBc Typ) 0.698 - 2.700 GHz make them ideal for in-building or tower top systems. Available 2-way and 3-way, 7/16 DIN and Type-N configurations.



Low PIM Adapters

MECA's Low PIM (-155 dBc Typ) Adapters for DAS Applications feature industry leading PIM performance of -160 dBc Min. Available in 7/16 DIN, Type N to SMA and 4.1/9.5 Mini-DIN connectors.



BETTER BUILDINGS / BETTER NETWORKS

Dr. D.A.S. © Prescribes: MECA Low PIM Products & Equipments
For next generation DAS there is only one name in passives.

It's simple. Better signals equal better performance. Today's buildings personify the need for next-level Distributed Antenna Systems (DAS). And the engineers that are building them turn to MECA for passive components. American ingenuity and 53 years of experience have resulted in the deepest, most reliable product line of ready-to-ship and quick-turn solutions, such as:

Power Dividers: Up to 16 way and 18 GHz

Attenuators: Up to 60dB and 500W

Terminations: Up to 500W

Couplers: Up to 40dB and 1kW

Integrated Rack Units: Delivered in 3-6 weeks

They come with an industry leading 3 year guarantee and true MECA pride. Ready to build a better DAS? Start with a visit to www.e-MECA.com.
"delivered on time every time!!"



Dr. D.A.S. © Prescribes...

Low PIM 250 Watt Terminations

Industry leading PIM performance of -165 dBc (Typ) and covering the 698 - 2700 MHz frequency bands available in Type-N, 7/16 DIN and 4.1/9.5 Mini-DIN, all in a 12" x 4.0" package. Ideal for IDAS / ODAS, In-Building, base station, wireless infrastructure, 4G, and AWS applications.



Integrated D.A.S. Equipment

Let MECA create an integrated assembly with any of our RF/Microwave products on 19" panels, shelves or NEMA enclosures.



MECA Electronics, Inc.

Microwave Equipment & Components of America

The Professional's Choice for RF/Microwave Passive Components

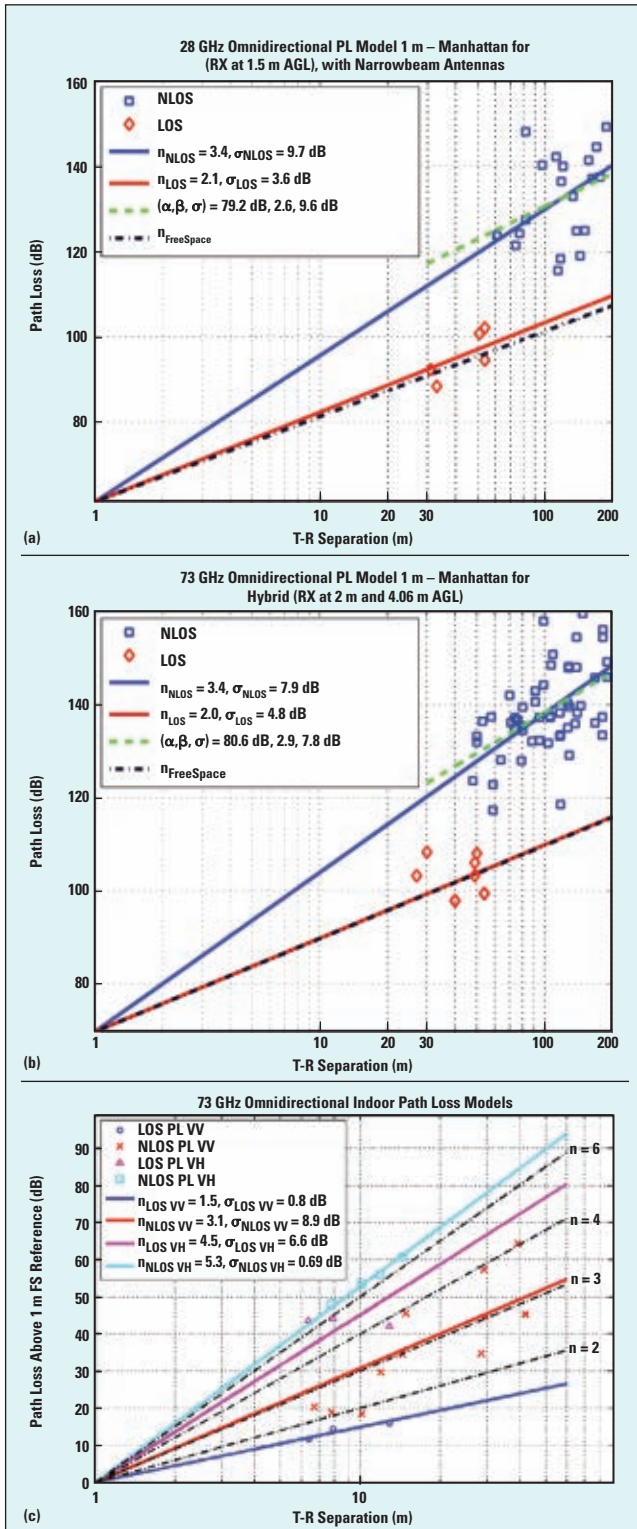
459 E. Main St., Denville, NJ 07834

Tel: 973-625-0661 Fax: 973-625-9277 Sales@e-MECA.com

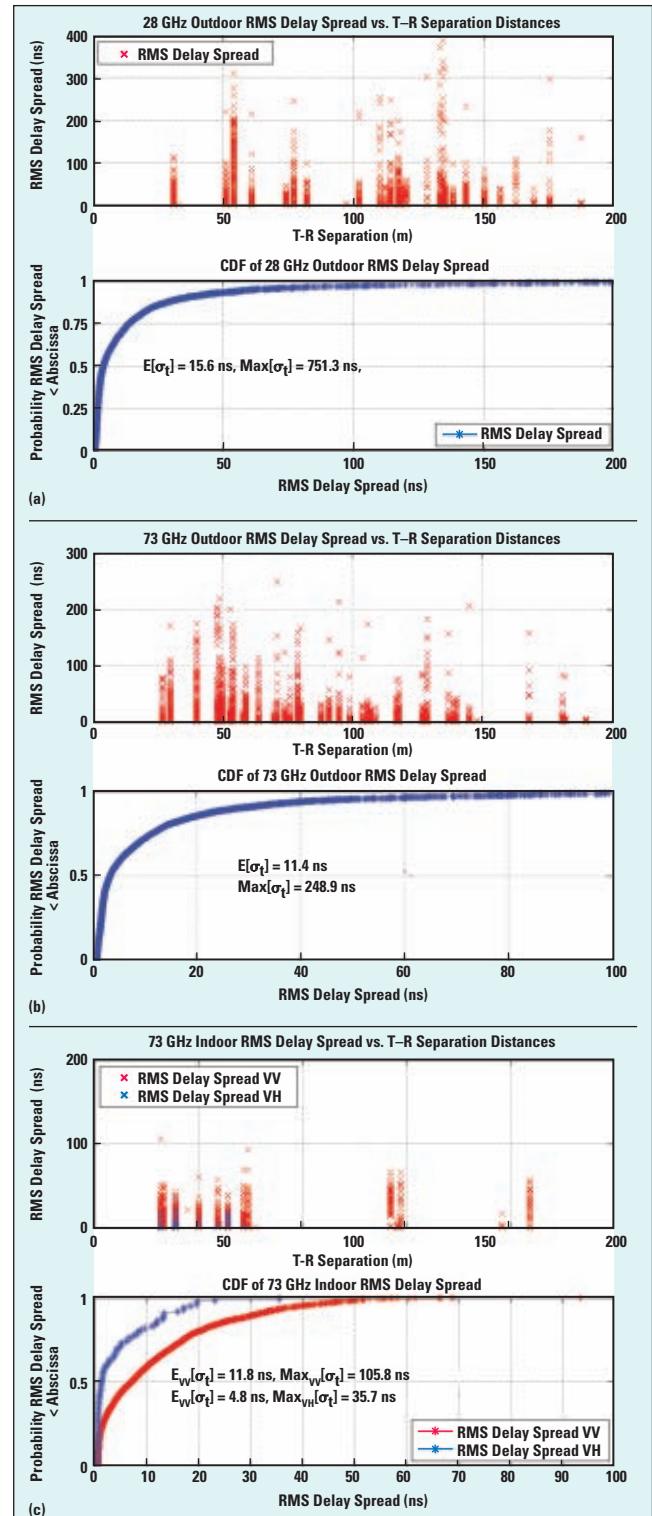


the multipath time dispersion of the channel used to estimate data rate and bandwidth limitations for multipath channels.^{3,4} To build power-efficient millimeter wave mo-

bile communication systems with simple equalization, the ideal situation is for particular beam pointing directions to offer both minimal path loss and minimal multipath delay spread. If the channel provides such paths, simplified receiver structures can be based solely on beamforming



▲ Fig. 7 28 GHz and 73 GHz close-in free space reference distance omnidirectional path loss in the outdoor urban environment of New York City, and indoor path loss models. 28 GHz outdoor omnidirectional path loss models (a). 73 GHz outdoor omnidirectional path loss models (b). 73 GHz indoor omnidirectional path loss models with VV and VH antenna polarization (c).



▲ Fig. 8 28 and 73 GHz RMS delay spread CDFs and RMS delay spread as function of Tx-Rx separation distance. 28 GHz outdoor measurements (a). 73 GHz outdoor measurements (b). 73 GHz indoor measurements (c).

TABLE 2

SUMMARY OF MINIMUM RMS DELAY SPREAD AND LOWEST PATH LOSS RESULTS FROM 28 GHz OUTDOOR AND 73 GHz OUTDOOR AND INDOOR MEASUREMENTS

Multipath Delay Spreads for the Directional Beams with the Minimum RMS Delay Spread							
Freq.	Scenario	Environment	Tx-Rx Separation Distance (m)	Path Loss (dB)	RMS Delay Spread (ns)	MED 10 dB (ns)	MED 20 dB (ns)
28 GHz	Outdoor	LOS	54	119.9	0.76	4.0	4.7
		NLOS	143	129.7	0.86	4.6	5.6
73 GHz	Outdoor	LOS	54	141.7	0.79	4.2	4.8
		NLOS	181	157.3	0.79	3.2	3.3
73 GHz	Indoor	LOS	6	141.5	0.54	2.1	2.1
		NLOS	29	86.3	0.56	1.9	1.9
Multipath Delay Spreads for the Directional Beams with the Lowest Path Loss							
28 GHz	Outdoor	LOS	33	88.4	0.84	4.5	5
		NLOS	114	126.2	165.10	7	1384.8
73 GHz	Outdoor	LOS	40	100.4	0.89	4.4	7.8
		NLOS	118	121.2	0.97	4.6	8
73 GHz	Indoor	LOS	6	86.3	0.85	4.6	5.3
		NLOS	10	90.7	0.80	4.4	5

and minimal equalization in the time domain, rather than using multi-tone, OFDM modulation and frequency domain equalization, as is done today.⁴

For this unique pointing angle scenario, **Figure 8** shows the RMS delay spread as a function of Tx-Rx separation and the associated cumulative distribution functions (CDFs) for 28 and 73 GHz outdoor and 73 GHz indoor measurements. The RMS delay spread in the 28 GHz outdoor measurements with 24.5 dBi gain narrow beam antennas shows that the majority of the multipath components arrive within about 50 ns. The RMS delay spread in the 73 GHz outdoor measurements with 27 dBi gain narrow beam antennas, combining backhaul and access scenarios, shows that a majority of the multipath components arrive within about 30 ns. For the 73 GHz indoor measurements, the majority of the multipath for co-polarized antennas arrives within about 35 ns, and for cross-polarized antennas within about 20 ns.

Generally, the RMS delay spread decreases as the Tx-Rx separation distance increases, since weaker components reaching the receiver at greater distances are not detectable above the receiver system's noise floor.²⁴

Table 2 summarizes Tx-Rx separation distance, path loss, RMS delay spread, maximum 10 dB down excess delay³ and maximum 20 dB down excess delay for specific antenna pointing angles. The characteristics are presented for two case-types in the table: values for one particular Tx-Rx angle pointing orientation that provides the minimum RMS Delay Spread for that case and values for one particular Tx-Rx angle pointing orientation that results in the minimum path loss, for the same Tx-Rx location combination. The values are determined from the entire measurement set that provided the smallest directional RMS delay spread and path loss.²¹⁻²³

A simple algorithm to find the best beam directions will help simultaneously minimize both RMS delay spread and path loss (i.e., finding the best paths for both maximum SNR and very simple equalization).²³ By selecting a beam with both low RMS delay spread and path loss, relatively high power can be received using directional antennas without complicated equalization, meaning that low latency single carrier (wideband) modulations may be viable candidates for future millimeter wave wireless systems. The measured values presented here are useful to the research community for

understanding values that may result when beamforming or beam searching algorithms are used to systematically search for the strongest Tx and Rx pointing angles, to achieve the lowest path loss or link attenuation.

CONCLUSION

This article describes the sliding correlator channel sounder system and presents the millimeter wave propagation measurements performed by NYU WIRELESS over the past two years. Results are shown for 28 GHz outdoor, 73 GHz outdoor base station-to-mobile (access), 73 GHz base station-to-base station (backhaul) and 73 GHz indoor scenarios. The measurement results include channel characteristics such as directional and omnidirectional path loss models relative to a 1 m free space reference distance, and directional delay spread.

The path loss model results obtained for unique pointing angles show that LOS free space propagation in outdoor ($n = 2.3$) and indoor environments ($n = 2.2$) for the 73 GHz band and outdoor environments ($n = 1.9$) for the 28 GHz band is favorable and close to the theoretical free space path loss ($n = 2$). The NLOS environment at 28 and 73 GHz experiences greater attenuation than the LOS environment yielding $n = 4.1$ for the 28 GHz outdoor directional measurements $n = 4.7$ for the 73 GHz outdoor scenario, and $n = 5.1$ for 73 GHz indoor measurements. However, with the use of multiple antenna elements, beamforming and beam combining technologies can significantly decrease the path loss when considering the best possible paths ($n = 3.7$ for 28 GHz outdoor, $n = 3.6$ for 73 GHz outdoor, and $n = 3.3$ for 73 GHz indoor co-polarization). The omnidirectional co-polarized path loss results are very promising for an indoor environment, as the LOS path loss exponent is smaller than for true free space, due to ground bounces and constructive interference from reflections.

RMS delay spread is generally inversely proportional to the Tx-Rx separation distance. Understanding RMS delay spread in the millimeter wave bands is important for wireless communications systems, especially where beam combining, beamforming and equalization are necessary to increase



the signal-to-noise ratio (SNR) and improve performance for a communication system.

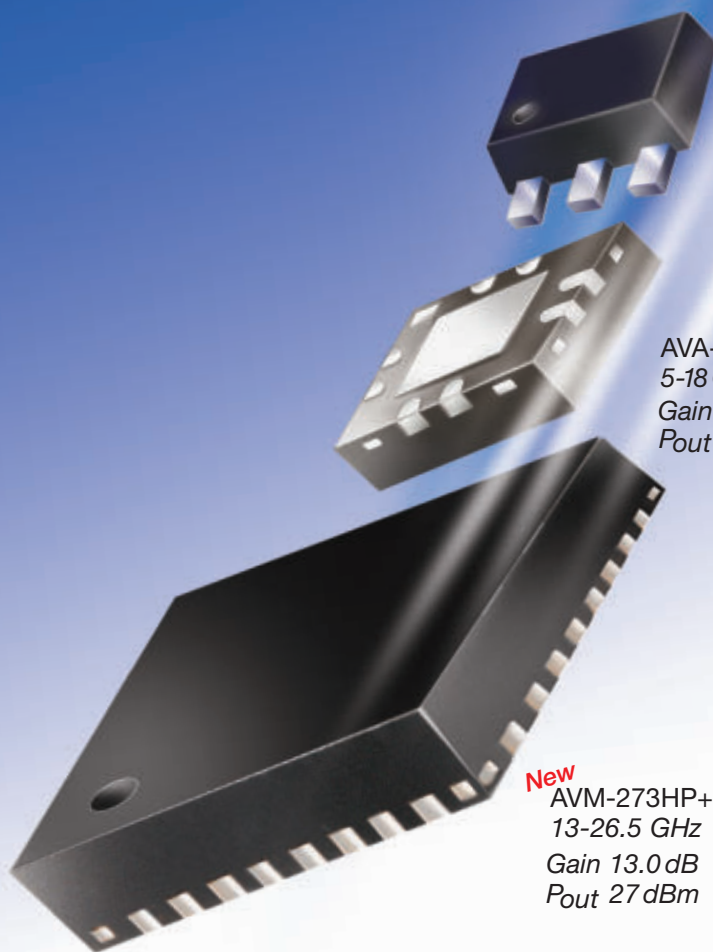
The data described in this article will allow for the development of statistical channel models for millimeter wave small cell wireless communications systems in dense urban environments. Statistical models in the form of 3GPP standards have already been published based on the measurements described.^{14,27,28} Given the large availability of spectrum at 28 and 73 GHz, millimeter wave bands will likely play a significant role in the next generation of cellular systems and these measurements and models will be an essential tool in their design. ■

References

1. T.S. Rappaport, J.N. Murdock and F. Gutierrez, "State of the Art in 60-GHz Integrated Circuits and Systems for Wireless Communications," *Proceedings of the IEEE*, August 2011, pp. 1390-1436.
2. A. Ghosh, T.A. Thomas, M.C. Cudak, R. Ratasuk, P. Moorut, F.W. Vook, T.S. Rappaport, G.R. MacCartney, S. Sun and S. Nie "Millimeter-Wave Enhanced Local Area Systems: A High-Data-Rate Approach for Future Wireless Networks," *Selected Areas in Communications, IEEE Journal*, pp. 1152-1163, June 2014.
3. T.S. Rappaport, *Wireless Communications: Principles and Practice*, 2nd ed. Upper Saddle River, NJ: Prentice Hall, 2002.
4. T.S. Rappaport, R.W. Heath Jr., R.C. Daniels and J.N. Murdock, *Millimeter Wave Wireless Communications*, Pearson/Prentice Hall, c. 2015.
5. T.S. Rappaport, S. Sun, R. Mayzus, H. Zhao, Y. Azar, K. Wang, G.N. Wong, J.K. Schulz, M.K. Samimi and F. Gutierrez, "Millimeter Wave Mobile Communications for 5G Cellular: It Will Work!" *IEEE Access*, pp. 335-349, 2013.
6. S. Rangan, T.S. Rappaport and E. Erkip, "Millimeter-Wave Cellular Wireless Networks: Potentials and Challenges," *Proceedings of the IEEE*, pp. 366-385, March 2014.
7. G.R. MacCartney, Jr., J. Zhang, S. Nie and T.S. Rappaport, "Path Loss Models for 5G Millimeter Wave Propagation Channels in Urban Microcells," *2013 IEEE Global Communications Conference (GLOBECOM)*, December 2013, pp. 3948-3953.
8. Y. Azar, G.N. Wong, K. Wang, R. Mayzus, J.K. Schulz, H. Zhao, F. Gutierrez, Jr., D. Hwang and T.S. Rappaport, "28 GHz Propagation Measurements for Outdoor Cellular Communications Using Steerable Beam Antennas in New York City," *2013 IEEE International Conference on Communications (ICC)*, June 2013, pp. 5143-5147.
9. M.K. Samimi, K. Wang, Y. Azar, G.N. Wong, R. Mayzus, H. Zhao, J.K. Schulz, S. Sun, F. Gutierrez, Jr. and T.S. Rappaport, "28 GHz Angle of Arrival and Angle of Departure Analysis for Outdoor Cellular Communications Using Steerable Beam Antennas in New York City," *2013 IEEE 77th Vehicular Technology Conference (VTC Spring)*, June 2013, pp. 1-6.
10. S. Nie, G. R. MacCartney, S. Sun and T. S. Rappaport, "73 GHz Millimeter Wave Indoor Measurements for Wireless and Backhaul Communications," *2013 IEEE 24th International Symposium on Personal Indoor and Mobile Radio Communications (PIMRC)*, September 8-11, 2013, pp. 2429-2433.
11. S. Sun, G.R. MacCartney Jr., M.K. Samimi, S. Nie and T.S. Rappaport, "Millimeter Wave Multi-Beam Antenna Combining for 5G Cellular Link Improvement in New York City," *2014 IEEE International Conference on Communications (ICC)*, June 2014.
12. G.R. MacCartney Jr. and T.S. Rappaport, "73 GHz Millimeter Wave Propagation Measurements for Outdoor Urban Mobile and Backhaul Communications in New York City," *2014 IEEE International Conference on Communications (ICC)*, June 2014.
13. S. Nie, G.R. MacCartney, S. Sun and T.S. Rappaport, "28 GHz and 73 GHz Signal Outage Study for Millimeter Wave Cellular and Backhaul Communications," *2014 IEEE International Conference on Communications (ICC)*, June 2014.
14. G.R. MacCartney, M.K. Samimi and T.S. Rappaport, "Omnidirectional Path Loss Models in New York City at 28 GHz and 73 GHz," *IEEE 2014 Personal Indoor and Mobile Radio Communications (PIMRC)*, September 2014, Washington, DC.
15. F. Gutierrez, S. Agarwal, K. Parrish and T.S. Rappaport, On-Chip Integrated Antenna Structures in CMOS for 60 GHz WPAN Systems, *IEEE Journal on Selected Areas in Communications*, Vol. 27, Issue 8, October 2009, pp. 1367-1378.
16. R.J. Pirkel and G.D. Durgin, "Optimal Sliding Correlator Channel Sounder Design," *IEEE Transactions on Wireless Communications*, September 2008, pp. 3488-3497.
17. D.C. Cox, "910 MHz Urban Mobile Radio Propagation: Multipath Characteristics in New York City," *IEEE Transactions on Vehicular Technology*, November 1973, pp. 104-110.
18. R.J. Pirkel and G.D. Durgin, "How to Build an Optimal Broadband Channel Sounder," *2007 IEEE Antennas and Propagation Society International Symposium*, June 2007, pp. 601-604.
19. G. Martin, "Wideband Channel Sounding Dynamic Range using a Sliding Correlator," *IEEE 2000 Vehicular Technology Conference Proceedings*, 2000, pp. 2517-2521.
20. E. Ben-Dor, T.S. Rappaport, Y. Qiao and S.J. Lauffenburger, "Millimeter-Wave 60 GHz Outdoor and Vehicle AOA Propagation Measurements Using a Broadband Channel Sounder," *2011 IEEE Global Telecommunications Conference (GLOBECOM 2011)*, December 5-9, 2011, p. 1-6.
21. S. Nie, M. K. Samimi, T. Wu, S. Deng, and T. S. Rappaport, "73 GHz Millimeter-Wave Indoor and Foliage Propagation Channel Measurements and Results," *NYU WIRELESS: Department of Electrical and Computer Engineering, NYU Polytechnic School of Engineering, Brooklyn, New York, Tech. Rep. 2014-003*, July 2004.
22. T.S. Rappaport, G.R. MacCartney Jr., M.K. Samimi and S. Sun, "Wideband Millimeter-Wave Propagation Measurements and Channel Models for Future Wireless Communication System Design" invited, *IEEE Transactions on Communications*, to be published.
23. S. Sun, T.S. Rappaport, R.W. Heath, A. Nix and S. Rangan, "MIMO for Millimeter Wave Wireless Communications: Beamforming, Spatial Multiplexing, or Both?" *IEEE Communications Magazine*, Vol. 52, No. 12, December 2014.
24. T.S. Rappaport and D.A. Hawbaker, "Wideband Microwave Propagation Parameters using Circular and Linear Polarized Antennas for Indoor Wireless Channels," *IEEE Transactions on Communications*, February 1992, pp. 240-245.
25. W.G. Newhall, T.S. Rappaport and D.G. Sweeney, "A Spread Spectrum Sliding Correlator System for Propagation Measurements," *RF Design*, April 1996, pp. 40-54.
26. T.S. Rappaport, E. Ben-Dor, J.N. Murdock and Y. Qiao, "38 GHz and 60 GHz Angle-Dependent Propagation for Cellular and Peer-to-Peer Wireless Communications," *2012 IEEE International Conference on Communications (ICC)*, June 2012, pp. 4568-4573.
27. T.A. Thomas, H.C. Nguyen, G.R. MacCartney Jr. and T.S. Rappaport, "3D mmWave Channel Model Proposal," *2014 IEEE Vehicular Technology Conference (VTC Fall)*, 80th, September 14-17, 2014.
28. M.K. Samimi, T.S. Rappaport, "Ultra-Wideband Statistical Channel Model for Non Line of Sight Millimeter-Wave Urban Channels," *IEEE Global Communications Conference, Exhibitions & Industry Forum (GLOBECOM)*, December 8-12, 2014.
29. T.S. Rappaport, E. Ben-Dor, J.N. Murdock, Y. Qiao and J. Tamir, "Cellular and Peer-to-Peer Broadband Millimeter Wave Outdoor Propagation Measurements and Angle of Arrival Characteristics using Adaptive Beam Steering," *IEEE Radio and Wireless Symposium (RWS) 2012*, Santa Clara, CA, January 15, 2012.
30. J.N. Murdock, E. Ben-Dor, Y. Qiao, J.I. Tamir and T.S. Rappaport, "A 38 GHz Cellular Outage Study for an Urban Outdoor Campus Environment," *IEEE Wireless Communications and Networking Conference (WCNC)*, April 2012.
31. A.I. Sulyman, A.T. Nassar, M.K. Samimi, G.R. MacCartney Jr., T.S. Rappaport and A. Alsanie, "Radio Propagation Path Loss Models for 5G Cellular Networks in the 28 GHz and 38 GHz Millimeter-Wave Bands," *IEEE Communications Magazine*, September 2014, Vol. 52, No. 9, pp. 78-86.
32. W. Hong, K.H. Baek, Y. Lee and Y. Kim, "Study and Prototyping of Practically Large-Scale mmWave Antenna Systems for 5G Cellular Devices," *IEEE Communications Magazine*, Vol. 52, No. 9, September 2014.

50 MHz to 26.5 GHz

THREE AMPLIFIERS COVER IT ALL!



PHA-1+ \$1⁹⁹
0.05-6 GHz ea. (qty. 20)
Gain 13.5 dB
P_{out} 22 dBm

AVA-183A+ \$6⁹⁵
5-18 GHz ea. (qty. 10)
Gain 14.0 dB
P_{out} 19 dBm

New
AVM-273HP+ \$27⁹⁵
13-26.5 GHz ea. (qty. 10)
Gain 13.0 dB
P_{out} 27 dBm

Mini-Circuits' New AVM-273HP+ wideband, 13 dB gain, unconditionally stable microwave amplifier supports applications from 13 to 26.5 GHz with 0.5W power handling! Gain flatness of ± 1.0 dB and 58 dB isolation make this tiny unit an outstanding buffer amplifier in P2P radios, military EW and radar, DBS, VSAT, and more! Its integrated application circuit provides reverse voltage protection, voltage sequencing, and current stabilization, all in one tiny package!

The AVA-183A+ delivers excellent gain flatness (± 1.0 dB) from 5 to 18 GHz with 38 dB isolation, and 19 dBm power handling. It is unconditionally stable and an ideal LO driver amplifier. Internal DC blocks, bias tee, and

microwave coupling capacitor simplify external circuits, minimizing your design time.

The PHA-1+ uses E-PHEMT technology to offer ultra-high dynamic range, low noise, and excellent IP3 performance, making it ideal for LTE and TD-SCDMA. Good input and output return loss across almost 7 octaves extend its use to CATV, wireless LANs, and base station infrastructure.

We've got you covered! Visit minicircuits.com for full specs, performance curves, and free data! These models are in stock and ready to ship today!

 RoHS compliant

FREE X-Parameters-Based
Non-Linear Simulation Models for ADS



<http://www.modelithics.com/mvp/Mini-Circuits.asp>





Scan page
using **layar** app

Understanding Envelope Tracking and Its Measurement Challenges

Yu Qian

*Keysight Technologies Inc., formerly Agilent Technologies electronic measurement business
Santa Rosa, Calif.*

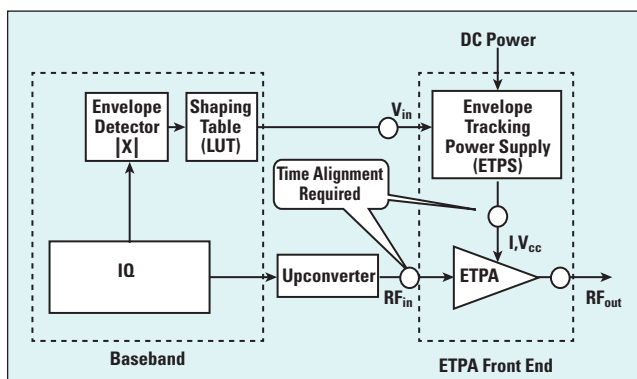
Power amplifiers (PA) are a critical component in mobile communication devices like smartphones and tablets. To increase data rates, mobile devices are operating ever wider bandwidths with multiple-input multiple-output (MIMO) data streams and higher-order modulation, and orthogonal frequency division multiplexing (OFDM). This requires the PA to achieve both better linearity and efficiency to ensure long battery life. Unfortunately, this

presents a bit of a problem for the PA, which is a power-hungry, nonlinear device. Fortunately, there is a technique that is helping overcome these issues: Envelope Tracking (ET). ET offers improved battery life and RF PA performance along with reduced heat dissipation. However, the technique is not without challenges. Let's take a closer look.

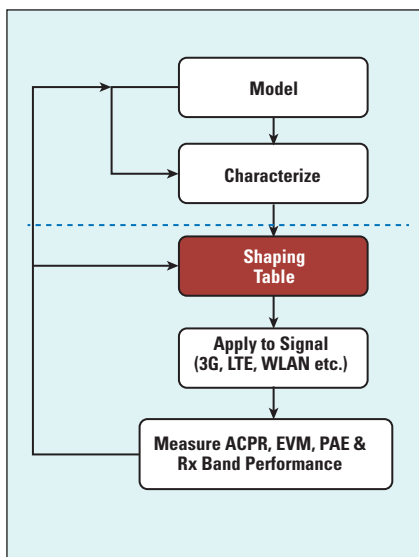
ET: THE BASICS

ET improves the power amplifier's efficiency by tracking its bias voltage with the magnitude of the input signal envelope. ET dynamically adjusts the DC power supply voltage based on the envelope of the PA input signal, enabling the amplifier to be more linear, reach higher peak power, and achieve greater spectral and power-added-efficiency (PAE). It also reduces issues associated with distortion.

A block diagram of a typical ET system is shown in **Figure 1**. Here, the envelope detector measures the magnitude of the IQ waveform, which is fed to a shaping table to determine the bias voltage supplied to the PA. The shaped envelope signal is supplied to the en-



▲ Fig. 1 Block diagram of a typical ET system.



▲ Fig. 2 Possible ET system design and test flow.

velope tracking power supply (ETPS), which modulates the bias voltage to track the RF input waveform. Finally, the PA amplifies the RF input signal.

ET does not apply a level limiter or operate with a fixed amplitude PA input signal, as is common with polar modulation. Instead, it may use a mixture of open and closed loop feedback, with delays introduced to the IQ or RF path to match those in the supply modulation path. In an open loop system, the shaping curve is applied to the envelope signal to match the supply voltage versus RF gain in the PA. Predistortion may also be used.

THE MEASUREMENT CHALLENGE

ET introduces an added complexity that makes configuring and testing an ET system especially challenging. Some of the specific challenges include:

PA Characterization for Simulation

ET requires additional testing, which drives up both test time and cost. A further complication, an ET PA must be treated as a 3-terminal active device. A low noise, high bandwidth power supply is also required, usually operating in a combination of switched and linear modes.

Shaping Table Design

The shaping curve or table determines the characteristics of the ET system. It must be properly designed and optimized to achieve the design goals, a process that is typically

lengthy and difficult, often requiring many steps. Once designed, the shaping table and all the other components required to implement an ET system (i.e., ETPS, RF PA and radio design) must be tested or evaluated.

Antenna Tuning

While tuning the antenna is often performed by a specialist, the designer will likely need to check the operation of the ET system with antenna mismatch.

Time-Aligned Signal Generation

A timing misalignment of the envelope and RF signals of more than 1 ns will adversely impact the quality of the transmitted signal, affecting both adjacent channel power (ACP) and error vector magnitude (EVM). Timing misalignment results in an asymmetric adjacent channel leakage ratio (ACLR).

AM/AM and AM/PM Measurement

While an ACLR measurement will show a problem with the ET system, it won't provide much insight into its cause. Linearity measurements of AM/AM and AM/PM, on the other hand, are key metrics for assessing ET performance. To improve linearity, supply modulation may be used. It reduces the in-band and out-of-band intermodulation signals at higher powers.

Instantaneous PAE

Measuring the improvement in system performance is a big challenge when implementing an ET system. The performance of the RF PA can be measured by itself, but it is a very difficult undertaking requiring measurement of the current with sufficient bandwidth. The supply current, voltage and RF power measurements need to be accurately time aligned to provide an instantaneous PAE measurement. An alternate and considerably easier approach is to measure the performance improvement as a combination of the ETPS and the ET PA, using a bench supply to measure average current.

Group Delay Through the ETPS

The ETPS has a lowpass filter response, making ripples in group delay through it especially worrisome. These ripples can cause excess distortion in the RF PA output.

Receive Band Noise Floor

In an ET system, all but the RF carrier decoupling capacitors are removed. Any spurious signals and noise on the power supply line to the RF PA appear at the output. Of particular concern is any increase in the transmitter noise floor that appears at the receiver duplex frequency in a frequency division duplexing (FDD) radio. This noise is coupled through the antenna duplexer and reduces the receiver's sensitivity.

In addition to these technical challenges, engineers must deal with the logistical challenge of determining which parts of the ET system to test and how to perform all of the modeling and measurement.

CONFRONTING THE CHALLENGES

Dealing with the challenges to implement an ET system requires two essential components. The first is an ET design and test flow. One possible flow is illustrated in **Figure 2**. It begins with modeling the PA's linear and nonlinear behavior and PA characterization. Next, the shaping table is designed. The envelope signal is then created, with the shaping table applied to the signal. Finally, the PA's PAE, ACLR and receive band performance are measured and analyzed.

The second element to evaluate ET components and ET-based radio designs is a highly flexible and accurate ET test system. Such a system should be comprised of a simulation environment, signal generator and analyzer with signal generation and analysis software, and an oscilloscope. For optimal flexibility, the system should support both LXI bench and PXI modular instruments and be based on common tools that enable effective teamwork, from R&D to design verification and into production.

A typical test system for the bench that can be used to perform the ET design and test flow is shown in **Figure 3**. For system modeling and simulation, electronic system level (ESL) design software is used to trade off the ET system's baseband and RF performance. The software allows customized models to be developed and shared prior to simulation, so the performance and impact of different devices can be understood.

To generate both the RF and en-



velope signals required for evaluation and performance testing of the ET system, signal generation software with an ET option is employed. Once the envelope waveform is created, it is downloaded to a vector signal generator. An arbitrary waveform generator is used to generate the envelope waveform signal.

After downloading the waveforms, the timing of the RF and envelope signals is adjusted with the signal generation software. An oscilloscope measures the absolute time delay. The entire ET system performance (RF signal, envelope signal, ETPS and RF PA) is then evaluated using a signal analyzer and associated software.

Based upon the results, the PA can be adjusted to improve its output signal quality, using ET alone or with other PA technologies like crest factor reduction (CFR) and digital pre-distortion (DPD). A general-purpose signal generator, signal analyzer and arbitrary waveform generator can help optimize PA performance.

PA characterization, including swept frequency and pulse power

measurements, is performed using a network analyzer and DC power analyzer with source measurement unit (SMU). If the DC power analyzer with SMU has a dynamic capability, pulsed PA performance may also be characterized. During PA testing, RF power modulation is measured using USB RF power sensors. A peak power analyzer and wideband sensor analyze the modulated power.

For production test, the following equipment is needed: waveform generation software, vector signal generator, arbitrary waveform generator, SMUs, digital inputs outputs (DIO) for device under test (DUT) control DC measurements, and a vector signal analyzer with appropriate measurement application software.

CONCLUSION

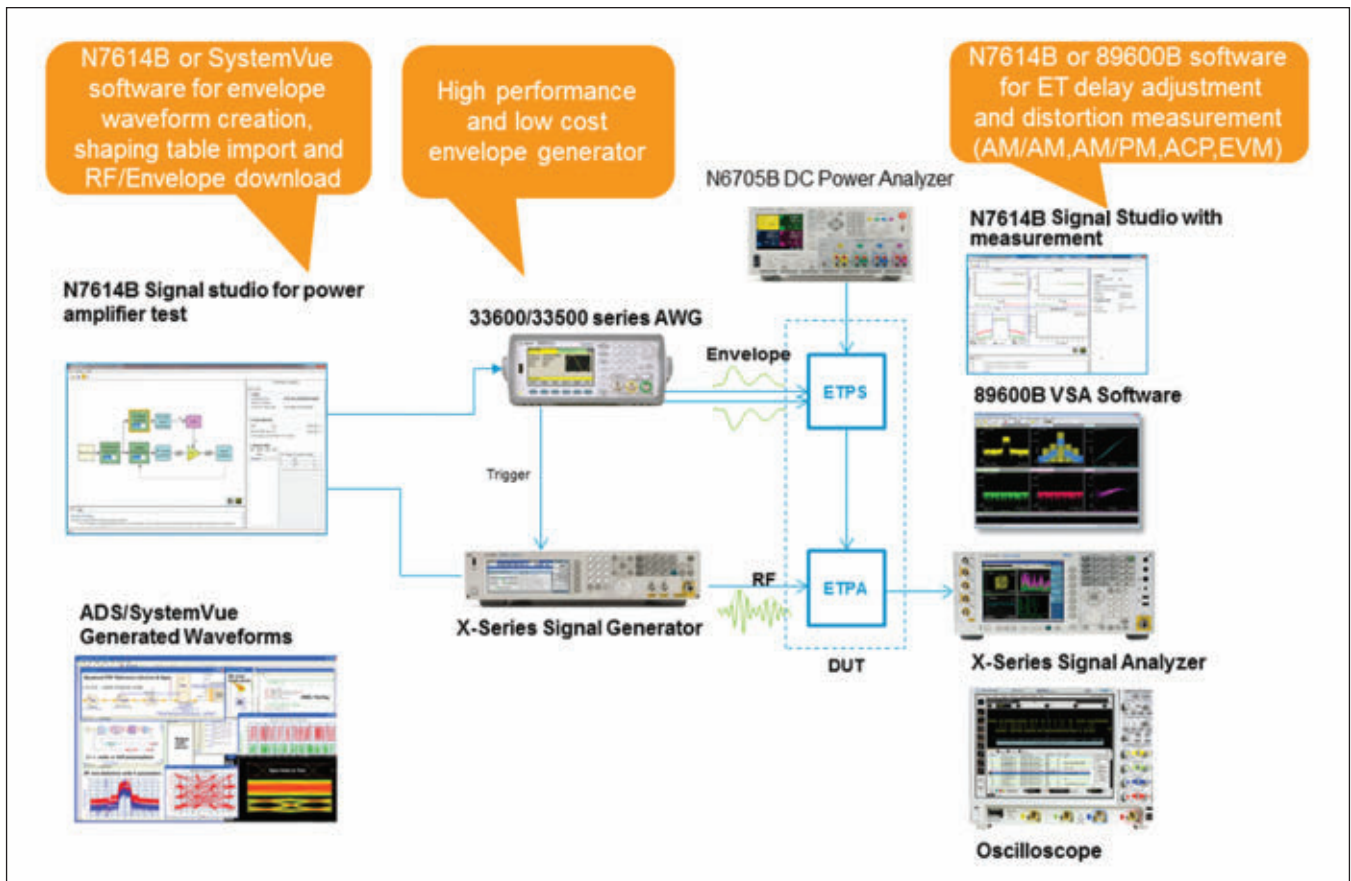
ET offers a number of performance advantages. However, to fully achieve these, designers must first understand and overcome the measurement challenges with configuring and testing an ET system. An accurate and flexible hardware/software test system speci-

cally targeted at ET combined with an ET design and test flow offer designers an ideal way to mitigate challenges that may arise. ■



Yu Qian (Kevin) is a wireless connectivity application expert and product marketing engineer with the Microwave Communications Division (MCD) at

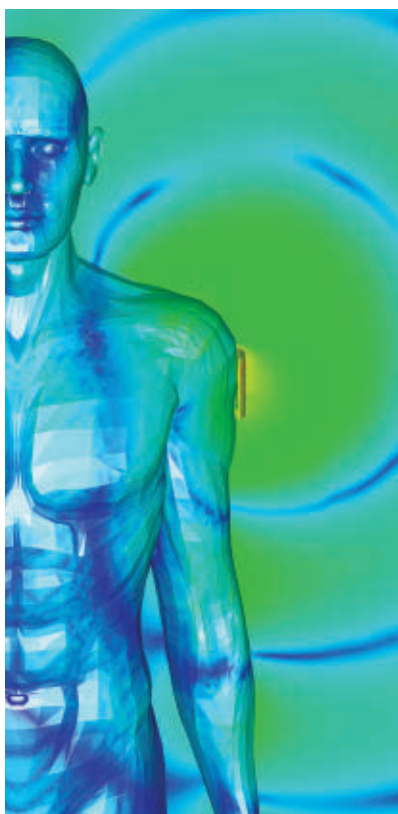
Keysight Technologies (formerly Agilent Technologies). Kevin has worked with Keysight for 13 years, with six years experience as an R&D software engineer and seven years experience as a marketing engineer and application expert. He is currently responsible for global wireless connectivity, new product introductions and business development. He also provides pre- and post-sale technical support and delivers training to internal field and application engineers and external customers. Kevin holds a master's degree in electrical engineering from Beijing University of Posts and Telecommunications (2001) and a bachelor's degree in electrical engineering from Shenyang Architecture University (1998).



▲ Fig. 3 A typical test solution for ET PAs.

Make the Connection

Find the simple way through complex
EM systems with CST STUDIO SUITE



Components don't exist in electromagnetic isolation. They influence their neighbors' performance. They are affected by the enclosure or structure around them. They are susceptible to outside influences. With System Assembly and Modeling, CST STUDIO SUITE helps optimize component and system performance.

Involved in antenna development? You can read about how CST technology is used to simulate antenna performance at www.cst.com/antenna.

If you're more interested in filters, couplers, planar and multilayer structures, we've a wide variety of worked application examples live on our website at www.cst.com/apps.

Get the big picture of what's really going on. Ensure your product and components perform in the toughest of environments.

Choose CST STUDIO SUITE –
Complete Technology for 3D EM.

CST SUCCESS STORY PULSE ELECTRONICS IMPROVES ANTENNA EVALUATION AND REDUCES PRODUCT DESIGN LEAD TIME WITH CST MICROWAVE STUDIO

Heikki Korva, Team Manager, RF, Pulse Electronics Wireless Division

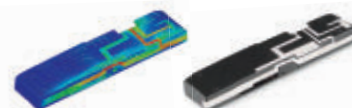


Figure 1: Antenna model, from simulation to mass production.

Pulse Electronics Mobile Division produces compact antennas for mobile communications and networking. Mobile antennas need to function in complex and mechanically limited environments, and so most antennas used today are specially designed and customer-specific.

About Pulse Electronics Wireless Division

Pulse Electronics Mobile Division produces compact antennas for mobile communications and networking. Mobile antennas need to function in complex and mechanically limited environments, and so most antennas used today are specially designed and customer-specific.

Our aim is to optimize antenna design for complex multi-radio environments, under all circumstances. The carefully developed Pulse solutions truly delight end users.

Pulse has delivered close to a billion antennas to the leading manufacturers of mobile devices. Pulse Wireless Division is headquartered in San Diego, USA, and has sites in Finland, China, South Korea, and Taiwan.

www.pulseelectronics.com

The antenna is one of the first electromechanical components considered in a new product concept design. In the past, most of the R&D work was done in the laboratory with the engineers constructing and testing different antenna designs for customer products. While this is still a good approach for single antenna systems, the introduction of UHF diversity schemes and other radio systems such as RF and GPS in current smartphones make reliable prototype evaluation very challenging.

Antenna prototypes typically include the device ground, PCBs, batteries, covers and any other large parts. Constructing early prototypes seldom include any active transmitters, and so each antenna must be placed in an external shielded cable. A typical UHF smartphone, with its main and diversity antennas, GPS and GSM/GPRS systems and a 2.4 GHz and 5.8 GHz WLAN capabilities, can need 5 or 8 cables to measure all the components at once. These cables would occupy too much of the volume of the prototypes, and severely distort the evaluation results. With electromagnetic simulation, the performance of a complete device can be calculated without worrying about these cable effects.

An example of an antenna product designed using only CST MICROWAVE STUDIO® (CST MWS) is shown in Figure 1.



www.cst.com

Find out how Pulse Electronics
improves antenna evaluation and
reduces product design lead time with
CST MICROWAVE STUDIO.





Scan page
using **layar** app

Six LTE Receiver Measurements Every Wireless Engineer Should Know

David A. Hall
National Instruments, Austin, Texas

From Wi-Fi devices to LTE handsets, today's wireless devices require several key measurements to characterize the ability of the receiver to demodulate an incoming signal from a base station or access point without distortion. Although many engineers are familiar with the notion of a sensitivity measurement (historically, the lowest signal level that can be received), this is just one of several measurements required to characterize receiver performance. There are actually six key measurements that engineers frequently use to evaluate receiver performance under a wide range of operating conditions.

Although this article describes these six receiver measurements in the context of an LTE receiver, the concepts apply to any wireless receiver. The 802.11 specifications are similar for wireless LAN radios.

LTE receiver metrics, shown in **Table 1**, are defined in section 7 of the 3GPP TS 36.521

specifications. Although Table 1 actually lists seven measurements, spurious response is functionally similar to blocking characteristics, so they'll be combined in this article.

When testing LTE receiver performance, the primary receiver figure of merit is receiver throughput. Each of the measurements listed in Table 1 defines conditions at which the device must meet minimum throughput requirements of 95 percent.

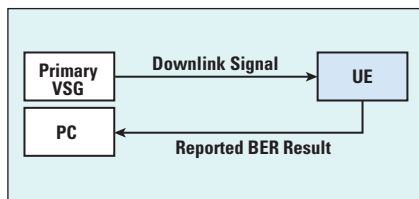
REFERENCE SENSITIVITY LEVEL

The reference sensitivity level describes the receiver's ability to operate within low signal power conditions. Unlike GSM and W-CDMA receivers that often use bit error rate (BER) to define the sensitivity requirements, LTE defines minimum performance in terms of throughput. Sensitivity is therefore defined as the lowest average power level at which the receiver can achieve 95 percent of the maximum throughput, when using QPSK modulation.

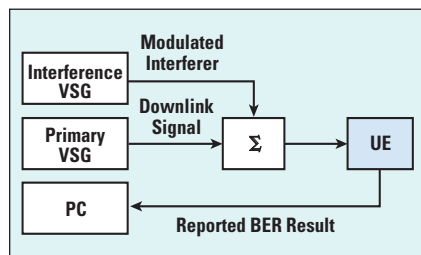
The hardware configuration for LTE reference sensitivity level requires a vector signal generator (VSG) directly connected to the receiver. It is common to use a fixed attenuator between the instrument and the device under test (DUT) or user equipment (UE) to improve the impedance match. As illustrated in **Figure 1**, the VSG produces an LTE downlink signal and the receiver reports its throughput through a digital interface.

The power level at which an LTE receiver must meet the required throughput varies according to the E-UTRA frequency band and

TABLE 1	
LTE RECEIVER MEASUREMENTS	
Measurement	3GPP TS 36.521 Section
Reference Sensitivity Level	Section 7.3
Maximum Input Level	Section 7.4
Adjacent Channel Selectivity	Section 7.5
Blocking Characteristics	Section 7.6
Spurious Response	Section 7.7
Intermodulation Characteristics	Section 7.8
Spurious Emissions	Section 7.9



▲ Fig. 1 Test setup for measuring LTE receiver sensitivity.



▲ Fig. 2 Test setup for measuring adjacent channel selectivity.

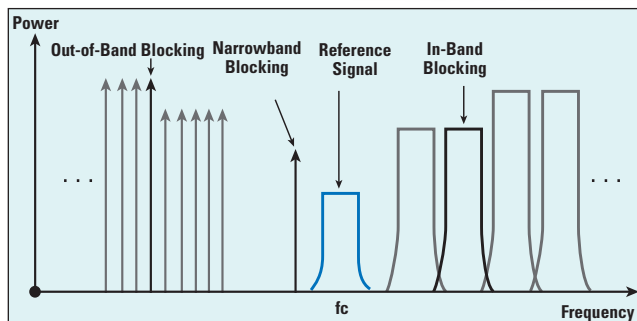
configured channel bandwidth. These conditions are defined in Table 7.3.3-1 of the 3GPP TS 36.521 specifications. The power levels range from -106.2 dBm for Bands 35 and 36 in a 1.4 MHz bandwidth to -90 dBm for Band 20 in a 20 MHz bandwidth.

MAXIMUM INPUT LEVEL

A second key metric of LTE receiver performance is maximum input level. Similar to the reference sensitivity level, the receiver's maximum input level characterizes its ability to achieve minimum requirements for throughput with large signal levels.

Receiver performance at relatively high power levels is primarily determined by the linearity of the front end, which is usually dominated by components such as the first LNA in the receive chain. The minimum conformance standards for maximum input level require that the receiver be able to achieve at least 95 percent of the maximum throughput in the presence of signal powers up to -25 dBm for all bands and in all channel bandwidths.

The test configuration for maximum input level is almost identical to reference sensitivity level. One minor difference is that it is not necessary to use substantial attenuation between the RF signal generator and the DUT when testing maximum input level. Instead, the signal generator is either connected directly to the DUT or through a small attenuator used for impedance matching.



▲ Fig. 3 Three types of interference signals are used to test the blocking characteristics of an LTE receiver.

ADJACENT CHANNEL SELECTIVITY

Adjacent channel selectivity (ACS) is a third metric for LTE receiver performance. ACS measures a receiver's ability to achieve minimum throughput requirements in the presence of an adjacent channel signal, i.e., at a specific frequency offset from the given channel. This measurement is particularly useful in determining the receiver's performance at the band edge, when higher power out-of-band signals from other base stations are present. ACS can strictly be defined as the ratio (in dB) of the receiver filter's attenuation at the assigned channel frequency to the attenuation at the adjacent channel.

The test configuration for ACS requires two signal generators connected to a power combiner. One VSG produces the reference LTE signal, which is demodulated by the receiver. The other signal generator produces the interfering LTE signal at an offset frequency, illustrated in **Figure 2**.

The outputs of both the primary downlink and interfering signal generators are combined to form a composite input to the UE. The specific requirements for LTE receiver ACS depend on the configured channel bandwidth and range from 33 dB in a 1.4 MHz channel to 27 dB in a 20 MHz channel.

Testing ACS generally involves two test configurations, one close to the sensitivity limit and one at the maximum input power to the receiver. When testing ACS at the lower end of the input power range, the primary RF signal generator generates a reference channel that is 14 dB above the receiver's sensitivity limits. The interfering RF signal generator produces an LTE signal at a higher output power, where the specific power

level depends on the bandwidth of the transmission.

When testing ACS at the higher end of the receiver's input power range, the interfering RF signal generator produces an interferer at the maximum input level of -25 dBm. Then, the primary RF signal

generator is configured to produce a reference channel that is substantially lower than the interfering signal. In this test, the absolute power level of the reference channel depends on the channel bandwidth.

BLOCKING CHARACTERISTICS

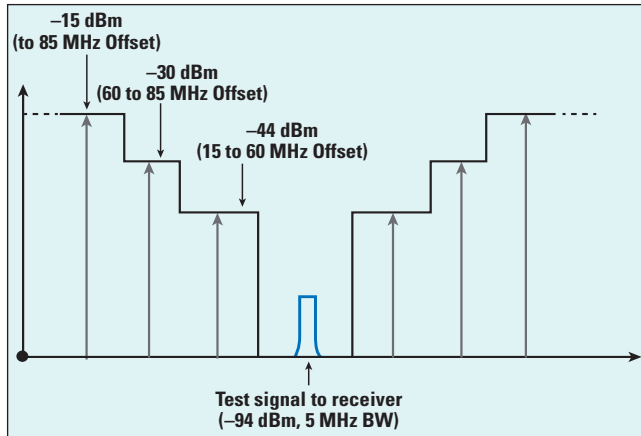
Blocking characteristics are a measure of the receiver's ability to accurately demodulate LTE signals in the presence of a wide range of interference. The specifications for LTE provide a more comprehensive range of interferers than the ACS measurement, including both continuous wave and modulated signals.

Figure 3 illustrates the range of blocking signals: continuous wave (CW) signals close to the band of interest (narrowband blocking), CW signals farther from the band of interest (out-of-band blocking) and modulated signals relatively close to the band of interest (in-band blocking).

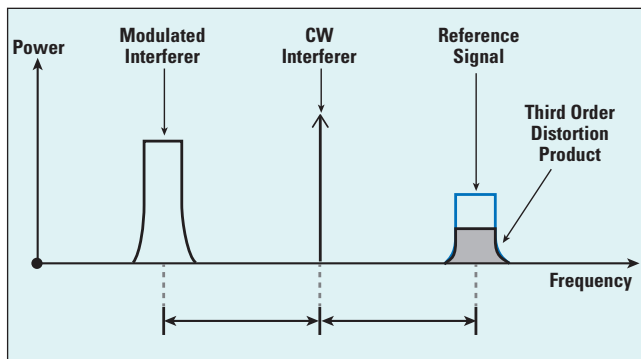
A test configuration similar to that used for ACS is used to measure blocking characteristics, i.e., combining the outputs of two RF signal generators. If the signal generator producing the interfering signal cannot generate CW and modulated signals, a separate CW signal generator will be required.

Similar to sensitivity and ACS, the blocking characteristics measurements require the receiver to achieve a minimum throughput of 95 percent of its maximum throughput for each of the in-band, out-of-band and narrowband blocking measurements.

In-band blocking is a metric measure of the receiver's performance in the presence of an unwanted interfering signal in the UE receive band or in the first 15 MHz below or above the receive band. When performing this measurement, the primary VSG is configured to produce an LTE signal



▲ Fig. 4 Power levels and frequency offsets for out-of-band blocking characteristics.



▲ Fig. 5 Interfering signals are spaced so the third order distortion product interferes with the reference signal.

6 to 9 dB above the reference sensitivity limit. The in-band interferer is a modulated LTE signal configured at either -56, -44 or -30 dBm, depending on frequency offset.

By comparison, out-of-band blocking characteristics evaluate the receiver's performance in the presence of higher power out-of-band signals. Unlike the in-band blocking characteristics that use a modulated signal, the out-of-band interfering signal is a CW signal at +6 dBm. When performing this measurement, the interference signal generator must be configured to generate a CW tone.

When testing out-of-band blocking, the reference LTE signal is generated at a power level that is 6 to 9 dB above the reference sensitivity level of the receiver, with the precise power level dependent on the bandwidth configuration. **Figure 4** shows that in the 5 MHz bandwidth configuration in E-UTRA Band 1, where the reference sensitivity requirement is -100 dBm, the test signal for out-of-band blocking is -94 dBm, which is 6 dB higher in power.

from 16 to 22 dB above the sensitivity level of the receiver. Also, the interferer is generated at a power level of -55 dBm for all bandwidth configurations and is spaced at a frequency offset that is just over 200 kHz away from the band edge of the signal of interest.

INTERMODULATION CHARACTERISTICS

Receiver intermodulation characteristics mimic the effect of the intermodulation products that occur in a receiver experiencing multiple interferers simultaneously. To perform this measurement, two interference signals are simultaneously injected, creating third-order distortion products that directly interfere with the reference downlink signal.

As shown in **Figure 5**, the frequency offset between the two interfering signals, both a CW interferer and a modulated interferer, is equivalent to the frequency spacing between the CW interferer and the reference signal to the receiver. Thus, the resulting third-order distortion product directly interferes with the reference signal.

The final blocking measurement, narrowband blocking, is a measure of the LTE receiver's ability to achieve minimum throughput in the presence of an unwanted narrowband interferer, where the frequency offset is less than the channel spacing. Similar to the out-of-band blocking measurement, the narrowband blocking requires a test configuration that uses both LTE and CW signals.

Because the interferer for narrowband blocking is close in frequency to the band of interest, the power level of the interferer is much closer to the power level of the reference signal. Here, the reference LTE signal ranges

The test setup for intermodulation characteristics requires three RF signal generators, two VSGs and one CW signal generator, and a three-way RF power combiner.

To pass the intermodulation characteristics measurement, a receiver must be able to achieve 95 percent throughput at power levels ranging from 6 to 12 dB above the sensitivity limit, depending on the channel bandwidth.

SPURIOUS EMISSIONS

The final critical LTE receiver measurement is spurious emissions. Unlike the other measurements, which define a receiver's ability to achieve a specified throughput under a range of signal conditions, the spurious emissions measurement characterizes the receive port's radiated emissions. It is the only receiver measurement that does not reference the throughput.

The hardware requirement for spurious emissions is straightforward and consists of connecting a spectrum analyzer to the receive port of the receiver. The spectrum analyzer measures emissions from 30 MHz to 12.75 GHz using a measurement bandwidth of either 100 kHz or 1 MHz (some exceptions apply to Bands 22, 42 and 43). The emissions requirement is -57 dBm in a 100 kHz bandwidth or -47 dBm in a 1 MHz bandwidth, with the measurement bandwidth dependent on frequency.

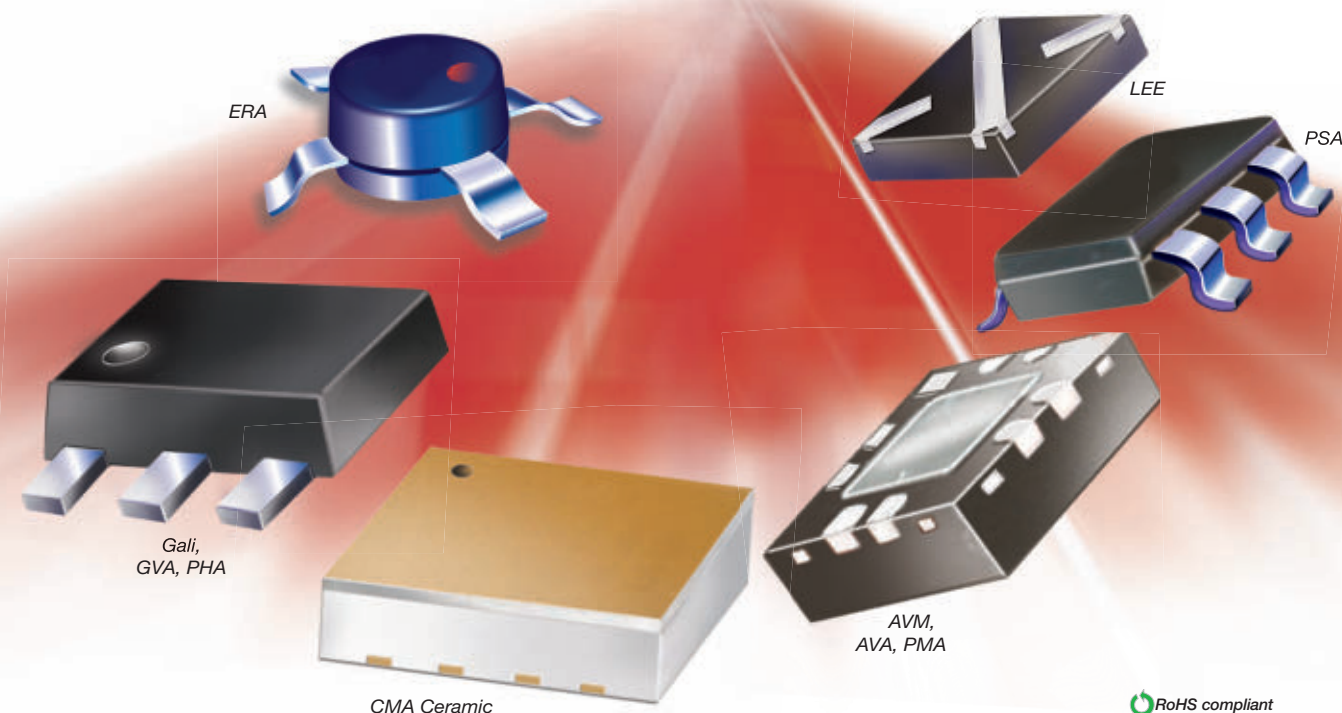
CONCLUSION

Although many engineers are most familiar with sensitivity as a metric for receiver performance, real-world environments require additional measurements. As the LTE receiver performance metrics indicate, receivers operate in the presence of a wide range of interfering signals that place requirements on both the noise floor and linearity performance. When testing an LTE radio for conformance with the 3GPP requirements, radio designers must consider a wide range of receiver performance metrics, from in-band emissions to intermodulation. ■

Note: This article is an abridged section from an application note entitled "Introduction to LTE Device Testing: From Theory to Transmitter and Receiver Measurements." For the full application note, visit: http://download.ni.com/evaluation/rf/Introduction_to_LTE_Device_Testing.pdf.

MMIC AMPLIFIERS

NOW!
DC to 26.5 GHz from **73¢** qty. 1000



RoHS compliant

NF from **0.5 dB**, **IP3** to **+48 dBm**, **Gain** from **8 to 39 dB**, **P_{out}** to **+30 dBm**

Now with over ¹⁷⁰~~145~~ MMIC amplifier models covering frequencies from DC to 26.5 GHz*, chances are, Mini-Circuits has your application covered. Our ultra-broadband InGaP HBT and PHEMT amplifiers offer one of the industry's broadest selections of gain, output power, IP3, and noise figure to optimize your commercial, industrial, or military system performance. They can even meet your most critical size and power requirements with supply voltages as low as 2.8V, current consumption as low as 16mA, and packages as small as SOT-363 (1.35 x 2.25mm). Our tight process control guarantees consistent performance across multiple production runs, so you can have confidence in every unit.

Visit minicircuits.com and use our Yoni2™ search engine to search our entire model database by performance criteria for the model that meets your needs. You'll find pricing, full model specs, characterization data, S-parameters, and even free samples of select models! So why wait? Place your order today, and have units in your hands as soon as tomorrow!

*Low-end frequency cut-off determined by external coupling capacitors and external bias choke.

Yoni2™ Searching millions of actual data points to meet your specific requirements.
U.S. Patents 7739260
7761442

EZ To Get SAMPLES
FREE Samples On Demand!
www.minicircuits.com/products/ez_samples.shtml

Mini-Circuits®

www.minicircuits.com P.O. Box 350166, Brooklyn, NY 11235-0003 (718) 934-4500 sales@minicircuits.com

476 Rev K



Design of an 8×8 MIMO Broadband RF Subsystem for Future WLAN

Li Zhao, Jian-Yi Zhou, Wen-Wen Yang, Zhi-Qiang Yu and Li-Na Cao
Southeast University, Nanjing, China

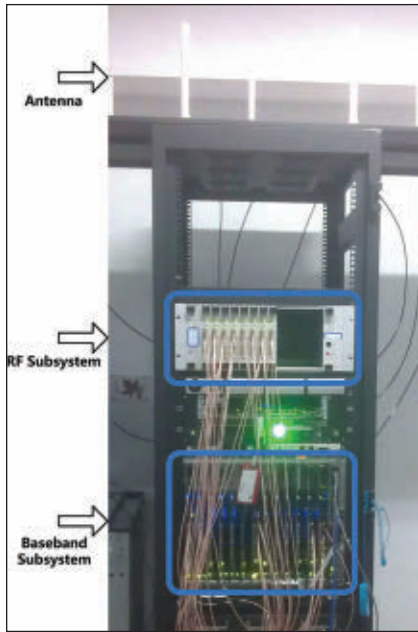
This article describes a broadband 8×8 MIMO RF subsystem with large area coverage for next generation wireless local area networks (WLAN) in the 5 GHz band. Measurements demonstrate the capability to operate over a long range of 80 m at a high data rate of 1 Gbps, due to its 23 dBm transmitter, -70 dBm sensitivity, 50 dB dynamic range receiver and 8 dBi high gain antenna. The EVM of transmitter and receiver are 2.6 and 3.2 percent, respectively, for an 80 MHz 64 QAM signal. The 8×8 RF subsystem has been successfully integrated into an IEEE 802.11ac prototype system. Because broadband OFDM signals employed in 802.11ac WLAN standards are more sensitive to non-ideal RF system characteristics such as phase noise, I/Q imbalance and interference, their effects are analyzed and mitigations are incorporated. Design details, fabrication considerations and measurement results are presented.

Increasing demand on high data rate, long range wireless communication networks has driven the advancement of wireless local area network (WLAN) standards. In 1999, 802.11b dictated a maximum data rate of 11 Mbps at 2.4 GHz, increasing to 54 Mbps at 5 GHz with 802.11a and at 2.4 GHz with 802.11g in 2003.¹ In 2009, 600 Mbps was achieved in 802.11n by using additional multiple-input-multiple-output (MIMO) antennas. With the continuing development of laptops and smartphones, however, there is a need for even larger amounts of data sharing,² driving the creation of a new standard for higher data rate WLAN. The new 802.11ac standard, also known as very high throughput (VHT), is capable of a 500 Mbps data rate with one spatial stream in the 5 GHz band and greater than 1 Gbps with multiple spatial streams. It benefits from new features, such as wider channel

bandwidth, a higher-order modulation scheme and more spatial streams.

There are three challenges in the design of an RF subsystem for future WLAN.³ First is the transceiver's higher sensitivity to I/Q imbalance and channel gain flatness due to its wide channel bandwidth. Second is a higher sensitivity to carrier frequency offset and phase noise than single carrier systems.⁴ Third is a higher peak-to-average ratio (PAR) caused by the complex modulation scheme, which requires more power back-off in the power amplifiers (PA).

Several methods are employed in this system to address these challenges and achieve excellent RF performance. Sufficient noise decoupling of the reference signal generation module and phase-locked loop (PLL) module improves the phase noise performance of the RF subsystem. The use of a broadband modu-



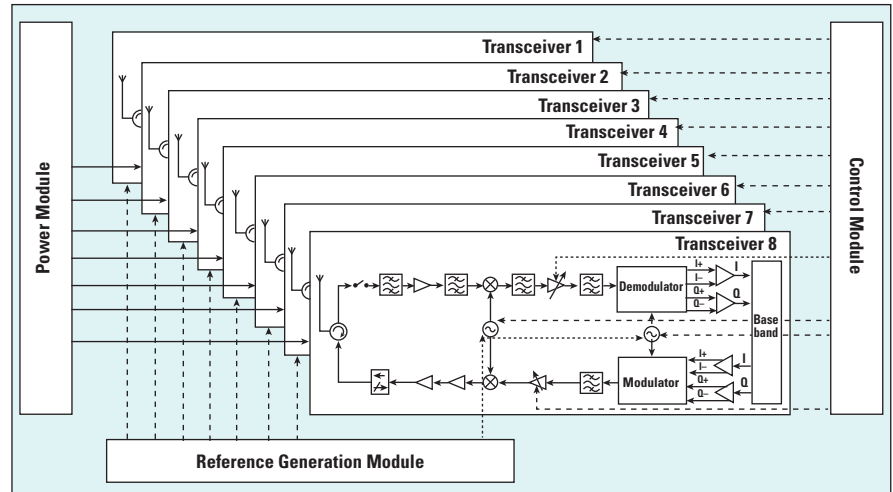
▲ Fig. 1 Hardware platform.

lators and extra operational amplifiers ensures good I/Q balance within the 80 MHz bandwidth. Close attention to the printed circuit board (PCB) layout and metallic shields between modules reduces interference.

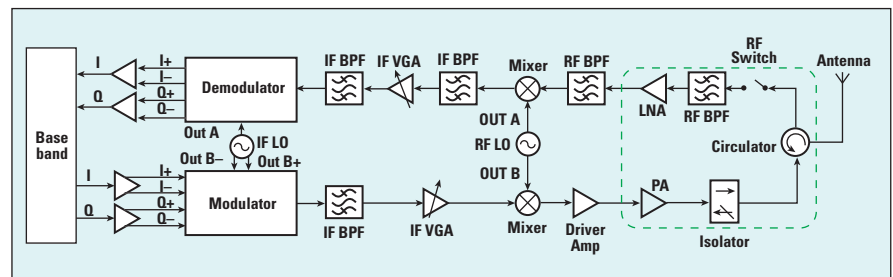
The measured communication range is as much as 80 m with a 1 Gbps data rate. Transmitter output power is as high as 23 dBm, which provides enough margin for the PA power back-off needed by the complex modulation scheme. The receiver operates over a large dynamic range of more than 50 dB. A parallel-fed twin-dipole array is used to form the 8 dBi high-gain antenna. The measured EVM of the transmitter and receiver using an 80 MHz 64 QAM signal is 2.6 and 3.2 percent, respectively.

SYSTEM OVERVIEW

The network is composed of one access point (AP) and user equipment (UE), which can be distributed throughout a building. The hardware platforms are the same at all the nodes (see **Figure 1**). The RF subsystem block diagram is shown in **Figure 2**. It has an operating frequency range of 5.76 to 5.84 GHz for an 80 MHz channel bandwidth and consists of one power module, one control module, one reference signal generation module and eight RF transceiver modules. The power module converts 48 to 6 VDC with a DC to DC converter. The control module guarantees communication between the baseband cir-



▲ Fig. 2 RF subsystem block diagram.



▲ Fig. 3 5.8 GHz WLAN RF transceiver block diagram.

cuitry and RF transceivers. The reference signal generation module, which consists of a 10 MHz oven controlled crystal oscillator (OCXO) and a PLL, provides a 10 MHz reference signal to each of the eight transceivers.

It works in a time-division-duplex (TDD) mode. The transceiver has an RF port to the antenna and an I/Q interface to the baseband. The peak-to-peak voltage of I/Q signals between the RF subsystem and baseband circuitry is 500 mV. The transmitter and receiver share one antenna by using a circulator as shown in **Figure 3**. Each transceiver has its own antenna, so there are eight antennas in total.

MITIGATION OF NON-IDEAL SYSTEM CHARACTERISTICS

Phase Noise

Improper setting of phase-locked loops (especially the loop filter bandwidth), a noisy power supply and reference frequency jitter are the main sources of phase noise. In the TDD mode, amplifiers on Tx and Rx paths are switched on and off with each communication burst in order to minimize power consumption. Power consumption changes dramatically between Rx mode and Tx mode, in-

roducing noise. Unless the noise is thoroughly decoupled, it can affect the crystal oscillator and cause jitter in the reference. Phase noise is reduced by properly setting the crystal oscillator loop filter bandwidth, using an ultra-low noise, low dropout, linear regulator in the PLL power supply and employing tantalum capacitors for further decoupling.

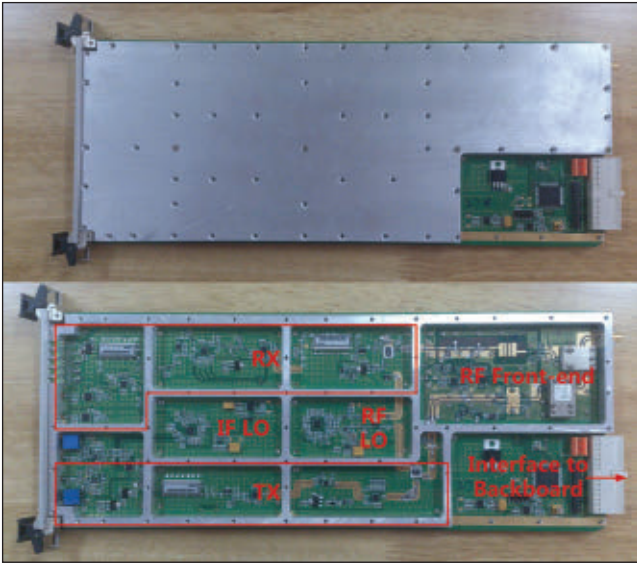
It is also important that the 10 MHz reference be distributed to each RF transceiver without introducing jitter, especially when multiple RF boards are inserted in the RF subsystem. This is accomplished with an ultra-low jitter LVC MOS fan-out buffer to distribute the reference to the eight RF transceivers.

I/Q Imbalance

Theoretically, a phase imbalance (θ) and an amplitude imbalance (β) degrade SNR according to⁵

$$SNR' = \frac{P_s}{P_N + P_{N\theta} + P_{N\alpha}} = \frac{SNR}{1 + SNR \left[\tan^2(\theta/2) + \alpha^2 \right]} \quad (1)$$

$$\text{where } \alpha = (10^{\beta/20} - 1) / (10^{\beta/20} + 1)$$



▲ Fig. 4 5.8 GHz WLAN RF transceiver prototype.

If SNR degradation of less than 2 dB is required to achieve an SNR = 21 dB, the phase imbalance should be less than 5 degrees and the amplitude imbalance should be less than 0.5 dB.⁶ In practice, I/Q imbalance has a greater impact on wide bandwidth systems.

Asymmetry in the PCB layout and different trace lengths for the baseband I and Q signals contribute to I/Q imbalance. For a modulator or demodulator, impurities in the LO signal also contribute to I/Q imbalance. A bandpass filter placed between the PLL and the demodulator can help to filter out undesired harmonics, while amplitude imbalance is compensated by adjusting the feedback resistor of the operational amplifier and phase imbalance is compensated by placing shunt capacitors in I/Q signal paths.⁷

Interference

Shielding between different parts of the RF transceiver is critical, especially those parts with large power.⁸ Different functional blocks are separated by a metal frame as shown in **Figure 4**. The large LO signal and its harmonics can be coupled to the RF front end through the dielectric substrate or other paths. To address this, LC lumped filters in the output path of the LO signal filter out the relatively high LO harmonics. A high isolation mixer is also used to reduce LO leakage.

Carrier feedthrough is mainly caused by imbalances in the DC offset between I/Q signals at the input of the modulator. The operational amplifiers shown in Figure 3 act as buffers between the baseband signals and the modulator, and can also provide DC offset compensation for the I/Q signals. Tuning the DC offset of the I/Q paths can effectively suppress the carrier feedthrough to a level below -55 dBc.

RF TRANSCEIVER AND ANTENNA DESIGN

Structure

The transceiver is integrated on a 1.5 mm thick, four-layer PCB.⁹ The first layer is on a Taconic TLX substrate, with $\epsilon_r = 2.55$, $h = 0.5$ mm. The others are on FR-4. The RF front end, shown in the green dashed line box in Figure 3, uses a two-layer PCB ($\epsilon_r = 2.55$, $h = 0.5$ mm) to provide

TABLE 1

TRANSCEIVER LINK BUDGET

Blocks		Specifications
Transmitter		
Modulator	P1dB	+ 9 dBm
	Image Suppression	> 35 dB
IF Amplifier and Filter	Gain	10 dB
	P1dB	+ 18 dBm
Mixer	Conversion Loss	7 dB
	IP3	+ 23 dBm
Driver	Gain	10 dB
	P1dB	+ 15 dBm
Power Amplifier	Gain	25 dB
	P1dB	+ 34 dBm
Transmitter	Flatness	< 1 dB
Receiver		
2-stage Low Noise Amplifier	Noise Figure	2.3 dB
	Gain	30 dB
	P1dB	+ 15 dBm
Mixer	Conversion Loss	7 dB
	IP3	+ 23 dBm
IF Amplifier and Channel Select Filter	AGC=0	AGC=60
	Gain: 60 dB	Gain: 30 dB
	Gain: 0 dB	
Demodulator	IP3	+ 18 dBm
	P1dB	+ 13 dBm
Receiver	Image Suppression	> 30 dB
	Flatness	< 1.5 dB
Antenna		
	IRL and ORL*	< 15 dB
	Gain	> 8 dBi

* IRL is the abbreviation of input return loss; ORL is the abbreviation of output return loss.

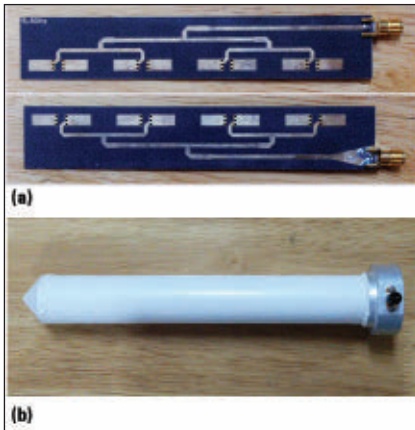
a good ground connection and proper heat dissipation for the PA. The two PCBs are fixed on one metal base and interconnected with adjacent microstrip lines. The RF band is from 5.76 to 5.84 GHz, with a 4.2 GHz LO frequency and a 1.6 GHz IF.

Link Budget

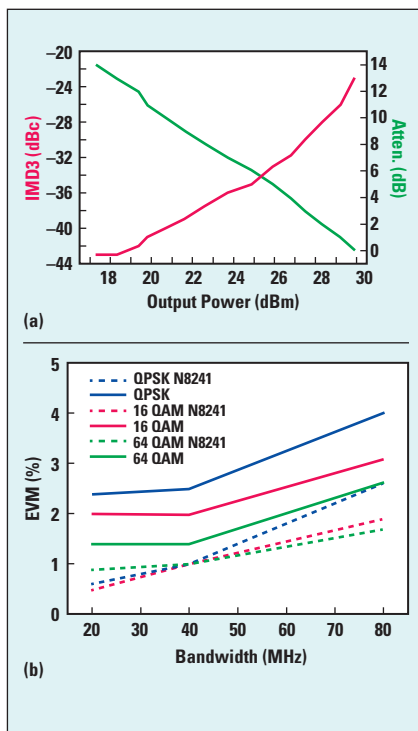
IEEE 802.11ac stipulates operation over 5 to 6 GHz with a 293 Mbps data rate (80 MHz bandwidth, 1 spatial stream, and 64 QAM 5/6) and a sensitivity of -58 dBm. The sensitivity for an 80 MHz QPSK signal is -71 dBm. The relation between sensitivity (P_{sen}), thermal noise (P_{noise}), noise figure (NF) and signal to noise ratio (SNR) can be expressed as

$$P_{sen} = P_{noise} + NF + SNR \quad (2)$$

A noise figure of 7 dB ($P_{noise} = -95$ dBm, SNR=17 dB for 80 MHz QPSK signal) is required to satisfy the -71 dBm condition. Gigabit-per-second data rates can be achieved by using multiple antennas and transceivers. The link budget



▲ Fig. 5 Antenna prototype (a) and its package (b).



▲ Fig. 6 Transmitter measured results; IMD3 (a) EVM at 23 dBm output power (b).

TABLE 2		
TRANSMITTER MEASUREMENTS		
Parameters		Measurement Results
LO Phase Noise	4.2 GHz	-83 dBc @ 1 kHz, -91 dBc @ 10 kHz, -102 dBc @ 100 kHz, -127 dBc @ 1 MHz
	1.6 GHz	-93 dBc @ 1 kHz, -98 dBc @ 10 kHz, -110 dBc @ 100 kHz, -135 dBc @ 1 MHz
Tx Output IM3		-36 dBc @ $P_{out} = +23$ dBm
Tx Gain Flatness		0.8 dB
Tx Carrier Suppression		> 55 dB
Tx Image Suppression		> 35 dB
Tx EVM (80 MHz QPSK)		4% @ $P_{out} = +23$ dBm
Tx SNR (80 MHz QPSK)		28 dB @ $P_{out} = +23$ dBm

of the transceiver is listed in **Table 1**.

Antenna

The high gain parallel-fed twin-dipole array antenna consists of four identical printed twin-dipoles with half wavelength separation. The two arms of the twin dipole are printed on each side of the substrate and connected by metal vias. This structure can also effectively suppress cross polarization. The feed network acts as a two-stage power divider. It is realized by parallel strips of the same width on each side of the substrate. When the feed lines are connected to different arms, the two dipoles have a 180 degree difference in phase, which means the dipoles work in the even mode.¹⁰ The antenna is fabricated on a 12.3×2.2 cm two-layer PCB, shown in **Figure 5a**, and is packaged in a plastic cylinder with a 3.5 mm SMA connector to the cable, shown in **Figure 5b**.

MEASUREMENT RESULTS

Performance is measured with a Keysight N8421A arbitrary waveform generator, R&S SMBV100A signal generator, Keysight N9020 spectrum analyzer and Keysight DSO91304A oscilloscope. Transmitter performance is summarized in **Table 2**, including phase noise of the local oscillator. Transmitter IMD3 and EVM performance is shown in **Figure 6**. Receiver performance is summarized in **Table 3**. Receiver EVM performance becomes worse with increasing bandwidth as

shown in **Figure 7**. The receiver's maximum input power is -20 dBm, and its minimum input power (sensitivity) is -70 dBm, resulting in a 50 dB dynamic range.

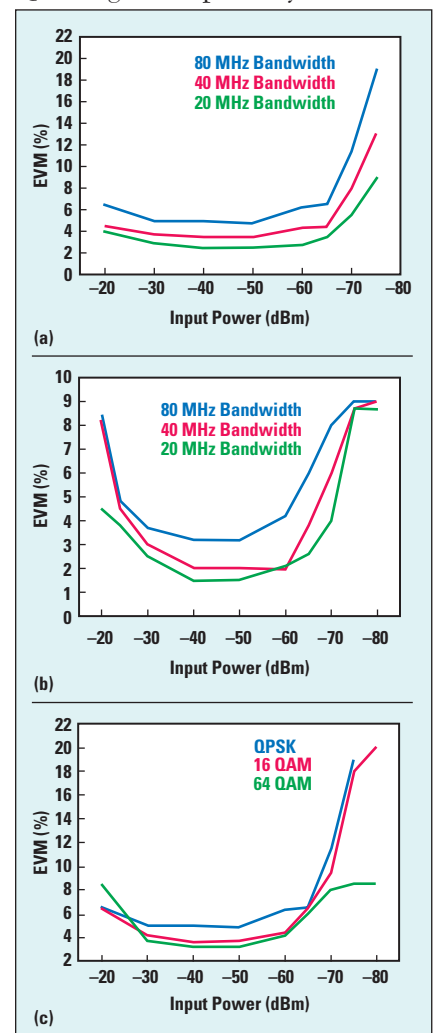
The arbitrary waveform generator creates the base-band signal, which is upconverted to 5.8 GHz by the signal generator. The transceiver is tested using

TABLE 3

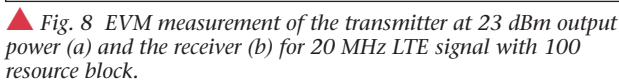
RECEIVER MEASUREMENTS

Parameters	Measurement Results
Rx Noise Figure	6 dB
Rx Gain Flatness	1.2 dB
Rx Dynamic Range	-20 to -70 dBm
Rx Image Suppression	> 35 dB
Rx EVM (80 MHz QPSK)	5% @ $P_{in} = -40$ dBm
Rx SNR (80 MHz QPSK)	26 dB @ $P_{in} = -40$ dBm

a 20 MHz LTE signal (which is also an OFDM signal) due to instrumentation bandwidth limitations. The measured transmitter and receiver EVM using the 20 MHz LTE signal is 2.1 and 2.2 percent, respectively (see **Figure 8**). Because of the lack of calibration for I/Q skew, EVM performance of the N8241A is poor (3.5, 2.4, and 2 percent for 80 MHz QPSK, 16 QAM, 64 QAM signal, respectively); therefore,



▲ Fig. 7 EVM performance of the receiver for QPSK signal (a) 64 QAM signal (b) 80 MHz signal (c).

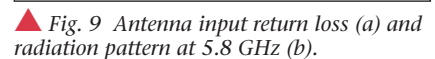


of coverage. ■

This work is supported in part by the National Natural Science Foundation of China under Grant 60702163, and in part by the National Science and Technology Major Project of China under Grant 2010ZX03007-002-01 and 2011ZX03004-003.

1. G. Hiertz, D. Denteneer, L. Stibor, Y. Zang, X.P. Costa and B. Walke, "The IEEE 802.11 Universe," *IEEE Communications Magazine*, Vol. 48, No. 1, January 2010, pp. 62-70.
2. Rolf de Vegt, "802.11ac Usage Models Document," IEEE, 802.11-09/0161r2, January 22, 2009.
3. Greg Jue, "Tackling MIMO Design and Test Challenges for 802.11ac

An RF subsystem for future WLAN has been designed, fabricated and measured. The influences of phase noise, I/Q imbalance and interference are analyzed, and measures are taken to provide performance improvements. The RF receiver has low noise, wide dynamic range and high image rejection within the broad channel bandwidth. The RF transmitter has a high IMD3 and low EVM at 23 dBm output power. The antenna has 8 dBi gain at 5.8 GHz. The 8×8 RF subsystem has been used in an IEEE 802.11ac prototype system successfully with more than 1 Gbps throughput over an 80 m radius



WLAN," *Microwave Journal*, Vol. 55, No. 3, March 2012, pp. 88-96.

- WLAN," *Microwave Journal*, Vol. 55, No. 3, March 2012, pp. 88-96.
4. T. Pollet, M. van Bladel and M. Moeneclaey, "BER Sensitivity of OFDM Systems to Carrier Frequency Offset and Wiener Phase Noise," *IEEE Transactions on Communications*, Vol. 43, No. 234, February/March/April 1995, pp. 191-193.
5. C.L. Liu, "Impacts of I/Q Imbalance on QPSK-OFDM-QAM Detection," *IEEE Transactions on Consumer Electronics*, Vol. 44, No. 3, August 1998, pp. 984-989.
6. L.H. Li, F.L. Lin and H.R. Chuang, "Complete RF-System Analysis of Direct Conversion Receiver (DCR) for 802.11a WLAN OFDM System," *IEEE Transactions on Vehicular Technology*, Vol. 56, No. 4, July 2007.
7. Z.Q. Yu, J.Y. Zhou, J.N. Zhao, T. Zhao and W. Hong, "Design of a Broadband MIMO RF Transmitter for Next-Generation Wireless Communication Systems," *Microwave Journal*, Vol. 53, No. 11, November 2010, pp. 22-26.
8. Z. Chen, W. Hong, J.Y. Zhou, J.X. Chen and C. Yu, "Design of Miniature RF Transceivers for Broadband MIMO Systems in Ku-Band," *Microwave Journal*, Vol. 55, No. 11, November 2012, pp. 108-116.
9. J. Hendricks, "Printed Circuit Board Materials for Microwave Designs in Automotive Applications," *Microwave Journal*, Vol. 50, No. 12, December 2007, pp. 84-94.
10. W. Hong, Q. Jiang, Twin Dipole Wideband Printed Antenna, patent: ZL00 2 20230.1. 2001.2.24.

Reactel, Incorporated

Reacting First to All Your Filter Needs.

DCS

WLL

MMDS

VHF

UHF



CDMA



Wireless

GSM

TX

Microcell

EGSM

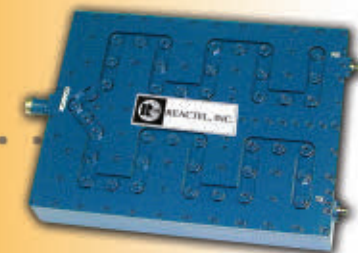
AMPS

& Mobile

UMTS

RX

WLAN



Cellular



SMR



Crossband Coupler

WiFi

PCS

AWS

- Submitting a request for immediate attention will never be easier.

- Full featured App contains expanded RFQ capability, catalog, data sheets and more.

- Available for iPad, iPod and Android devices via the App Store and Google Play.



3G

8031 Cessna Avenue • Gaithersburg, Maryland 20879 • Phone: (301) 519-3660
For general inquiries, please email reactel@reactel.com • <http://twitter.com/reacteljim>
Go online to www.reactel.com to download your Reactel catalog today.



@reacteljim



Smart Antennas and Front End Modules in Q-Band for Backhaul Networks

R. Vilar, J. Marti

Universitat Politecnica de Valencia

R. Czarny

Thales Research and Technology

M. Sypek, M. Makowski

Ortech SP. Z O.O.

C. Martel, T. Crépin, F. Boust

Office National d'Etudes et de Recherches Aerospatiales

R. Joseph, K. Herbertz, T. Bertuch

Fraunhofer Institute for High Frequency Physics and Radar Techniques FHR

A. LeFevre

Thales Communications & Security SA

F. Magne

Bluwan Ltd.

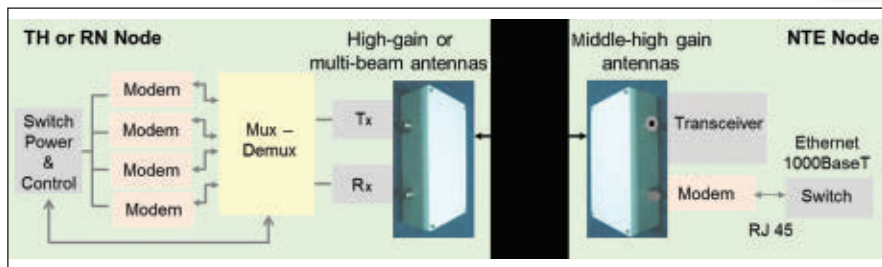
As mobile operators face increasing base station density as well as growing bandwidth requirements, mobile backhaul has become the new challenge. This article defines the architecture for future mobile backhaul networks as proposed in the framework of the FP7 EU SARABAND project. The solution exploits a new and wider frequency band, Q-Band (40.5 to 43.5 GHz), to provide massive capacity. Since full deployment of Q-Band backhaul networks requires new technology development, an overview of disruptive antenna and front end technology developed within this project is also provided.

Demand for bandwidth is growing exponentially as consumers use their mobile devices in more bandwidth-intensive applications. The evolution to 3G and 4G/LTE mobile technologies provides a path to more efficient use of the radio spectrum and progressively higher uplink and downlink speeds to each user. Operators' forecasts show that additional steps are required to provide sufficient bandwidth.

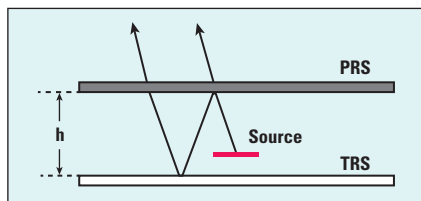
As a result, operators have begun to intro-

duce small cells into their networks, since this solution has recently emerged as a more cost-effective way for network mobile operators to improve the coverage and capacity of their mobile services. But there are some challenges to leveraging the benefits of small cells. One of the most significant is providing scalable, flexible mobile backhaul to connect small cells back into the network without breaking the small cell business case.

Operators typically use different backhaul



▲ Fig. 1 Network node architecture.



▲ Fig. 2 Fabry-Perot cavity.

technologies for their radio access networks. Nevertheless, existing alternatives such as fiber, digital subscriber line (DSL) and microwave backhaul do not provide the required CAPEX, OPEX and/or performance; therefore, an adequate backhaul upgrade in capacity and cost-efficiency is required. Millimeter wave technology, especially in Q-Band (40.5 to 43.5 GHz), offers a wide frequency spectrum, compactness and lightness of equipment and ease of implementing interference-free system configurations. This makes it very promising for high data rate backhaul applications.

The SARABAND project integrates Q-Band millimeter wave technology for point to multipoint (PMP) transmission to provide a cost-effective solution capable of supplying 150 to 200 Mbps per cell site.

WIRELESS BACKHAUL ARCHITECTURE

The wireless backhaul architecture proposed in SARABAND is a hierarchical, PMP Ethernet-based network composed of nodes linked by radio transmissions and remotely managed by a backhaul network management system (NMS). The solution is a distribution tree connecting a service provider's point of presence (PoP) to relay nodes ultimately reaching subscriber terminals, grouped terminals and mobile base stations. The main features are:

- A highly flexible PMP network topology that rapidly adapts to an operator's coverage and capacity requirements while simplifying radio deployment.

- The use of Q-Band, providing a large spectral bandwidth suitable for wide channels (40.5 to 43.5 GHz in 1 GHz sub-bands).
- A radio backhaul network composed of a multiplex of channels that aggregates several 100 Mbps half-duplex (TDD) channels to provide the required throughput (up to 2 Gbps half-duplex per 1 GHz radio transmission).
- Layer 1 and 2 of the network based on the 802.11n and then the 802.11ac standards and aggregation on 802.3ad.

The backhaul network architecture is composed of different types of nodes (see **Figure 1**). The Transmission Hub (TH) carries traffic in the core network and connects several terminals or relay nodes (RN). Relay Nodes extend system range and avoid the limitations of line of sight. Network Terminal Equipment (NTE) delivers basic services to customers' points of presence.

To enable any configuration of hierarchical PMP links while meeting the required performance on each segment of the network, the SARABAND project is developing new Q-Band backhaul network technology to increase network node throughput, range and coverage, while reducing cost. Specific developments include:

- Q-Band low-profile, high-gain antennas that will enhance throughput between the TH and the remote sites. Two approaches have been analyzed: Fabry-Perot antennas and lens antennas for medium-gain (20 dBi) and high-gain (>30 dBi) applications, respectively.
- Q-Band programmable multi-beam antennas, which will enhance coverage, reduce interference and save energy. Circular Switched Parasitic Array (CSPA) antennas, for an agile antenna solution, have been analyzed.
- Q-Band miniaturized radio modules

TABLE 1

FP ANTENNA SPECIFICATIONS

Size	70 × 70 mm
Height	7 mm
Gain	16 to 25 dBi
Beamwidth -3 dB (E/H planes)	15° / 15°
Bandwidth at -10 dB	1 GHz
Side lobe levels vs main lobe	-13 dB

based on new substrate, packaging and interconnection processes with the objective of providing modules with low loss, high power and high reliability at a fraction of the price of any currently available radio.

FABRY-PEROT ANTENNA

A Fabry-Perot (FP) antenna is a planar structure providing highly directive beams with properties such as a low profile, lightweight, simple feed mechanism and low cost. This makes it a good candidate to address Q-Band medium gain coverage requirements.

The FP antenna (see **Figure 2**) is a type of leaky wave antenna, consisting of a partially reflective surface (PRS) at a proper distance from a totally reflective surface (TRS). The resulting cavity may be filled with air or a dielectric material and is excited by a source that is placed inside the cavity.¹ With an appropriate design, parallel plate modes are excited in the cavity by the source. The power carried by the modes leaks through the PRS, forming a broadside pencil beam in the far field. The distance between the two reflecting surfaces (h) of the cavity and the source position are important antenna parameters.

Considering that the source is positioned at the same level as the PRS, the power radiated in the boresight direction is at a maximum when the following condition is satisfied:

$$\phi_R + \psi_R - \frac{2\pi}{\lambda} \cdot 2h = 2n\pi \quad (1)$$

where ϕ_R is the reflection phase of the PRS, ψ_R is the reflection phase of the TRS, h is the Fabry-Perot cavity height, and $n = 0, 1, 2, 3, \dots$

For the SARABAND project, the FP antenna specifications are shown in **Table 1**. It uses an air-filled FP cavity to reduce losses and provide the best compromise for maximum di-

TABLE 2

LENS ANTENNA SPECIFICATIONS

Size	< 250 mm (f/D < 0.5)	< 150 mm (f/D < 0.5)
Gain	> 35 dBi	> 30 dBi
Beamwidth -3 dB	< 3° horizontal and vertical	< 5° horizontal and vertical
Bandwidth at -10 dB	3 GHz (or 1 GHz centered in each Q-Band)	
Diffused lobes	Mean value < 30 dB between 45° and 90°	

rectivity and pattern bandwidth. The PRS is made of periodic patches (2.88×2.88 mm with a 4.2 mm square periodicity) printed on a 0.51 mm thick dielectric substrate placed 2.79 mm above the TRS. A patch within the air-filled cavity is the source of excitation.

An FP antenna produces a highly directive beam with a single feed source, where

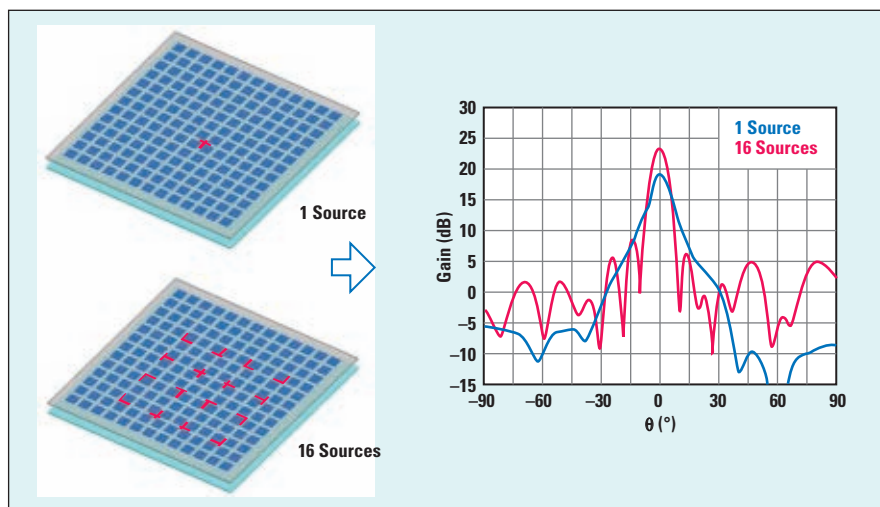
$$\text{directivity}(D) = \left(4\pi / \lambda^2\right) A \quad (2)$$

for an aperture with an area A . While it is possible to reach up to 90 percent of the theoretical maximal directivity with a few lambda size aperture and a highly reflecting PRS, practical realizations achieve directivities around 50 percent of this limit.

FP antennas, however, are narrowband. Jackson et al.,¹ have shown that for a simplified configuration, the product of directivity and 3 dB bandwidth is a constant that can be estimated by the formula:

$$D \cdot \text{BW} \approx \frac{2.5}{n^2} \quad (3)$$

with n being the cavity refraction index.



▲ Fig. 3 FP antenna gain in the E-plane.

The high-gain antenna for the SARABAND project requires a 7.2 percent fractional bandwidth. Basic FP antennas have a fixed directivity-bandwidth product insufficient to meet this requirement; however, the gain can be increased through several complementary means. One is to extend the size of the radiating aperture making the surface through which the leaky wave radiates electrically large, achieving medium to high gain. Typically the PRS can be extended to a size of about $10 \times 10 \lambda$. A larger PRS size may not lead to a further gain increase since energy usually leaks from the cavity area being close to the source.

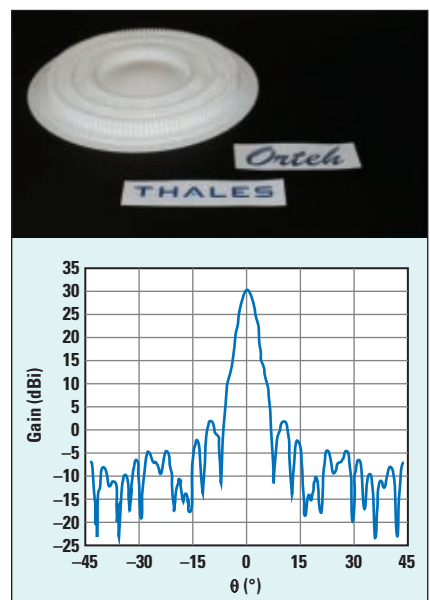
Antenna gain can be further increased by using multiple sources inside the cavity, making more efficient use of the large radiating surface. Furthermore, due to the presence of the PRS, the sources can be spaced 1.5λ apart without generating grating lobes in the radiation pattern. This excitation mechanism requires a small feed network to distribute the energy between the multiple sources. **Figure 3** shows FP antennas with 1 and 16 sources, which have been designed to provide maximum gain. In both cases, the antenna size is 60×60 mm ($\sim 8.3 \times 8.3 \lambda$ at 41.5 GHz). Maximum gain is achieved at 41.5 GHz with 1 source (19.2 dBi) and 41.75 GHz with 16 sources (23.3 dBi).

LENS ANTENNAS

In lens antennas, a quasi-point source (the feed) generates a spherical wave which is collected and collimated by a dielectric lens. This results in a plane wave at the antenna output that may provide diffraction-limited gain. Current lens antenna technology is either bulky (refractive design) or low-profile but less efficient (e.g., Fresnel lens).² To achieve a lower profile, yet efficient design, an innovative lens based on “quasi-optical” RF components is being investigated. It is the transposition of an optical approach, in terms of wavefront control and component design, to the RF domain. This enables the synthesis of an efficient, flat, high numerical aperture lens for controlling and reshaping the wavefront emitted by the Q-Band antenna feed.

Lens antenna operation is based on diffraction and constructive interference between zones composing the lens. The use of sub-wavelength structures and a hybrid lens design overcomes the usual Fresnel-lens limitations and does not suffer from loss of efficiency and bandwidth reduction when implemented in a low-profile configuration.

For the SARABAND project, this approach is applied to two different antennas of different sizes in order to cover both TH and NTE requirements. Specifications for the high-gain lens antennas are shown in **Table 2**. The distance between feed and



▲ Fig. 4 Simulated gain of a low-profile high-gain lens in the H-plane at 42 GHz.




Anaren Precision Etched Ceramics (APECS) — offering thin-film tolerances & performance, at a thick-film price



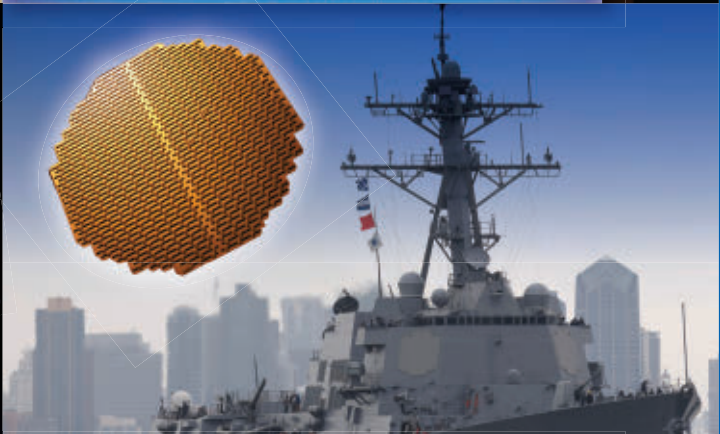
Space/Mil-grade Xinger® couplers — proven in Mars missions & ready for tough terrestrial settings, too

1 billion
Xinger
components
sold!

First on genuine Xinger-brand components!



Space-qualified couplers & power dividers — high-rel, lightweight & low-power for today's satellite applications



RF solutions for next-gen AESAs — including manifolds, T/R modules & beam-formers for air, sea, and land platforms

Isn't it time to put Anaren innovations like these to work for you?

Fast-approaching our 50th anniversary — and this year celebrating our 1 billionth Xinger®-brand coupler sold! — today's Anaren continues to drive innovative, best-in-class RF technology for the world's most demanding space, defense, wireless, and consumer electronics customers.

- > **Our Space & Defense Group** offers a fast-growing range of passive and active solutions, including multichip modules, IMAs, and custom solutions for today's digital radars. Exciting, new PCB and ceramic substrates and multilayer packaging techniques. And a growing line-up of space-grade components and high-temperature modules.
- > **Our Wireless Group** continues to reinvent the passive components category. From new, Femto-sized and mil-grade Xinger®-brand SMTs. To subminiature baluns and couplers for consumer products. To our growing family of Anaren Integrated Radio (AIR) modules and other solutions for the wireless IoT.

To learn more about how today's Anaren can make you more competitive tomorrow — visit www.anaren.com or email us at sales@anaren.com today!



Anaren®

What'll we think of next?®

800-411-6596 > www.anaren.com



lens must be optimized to take into account the feed radiation pattern, the lens size and the local sub-wavelength structure. For a given antenna volume, we can compute the configuration giving the highest antenna efficiency and therefore the highest gain. An example is shown in **Figure 4**.

CSPA ANTENNA

An attractive concept for electronic beam steering is the circular switched parasitic array (CSPA) antenna, which is proposed for the agile Q-Band antenna with a large field of view to be used in the repeaters. The basis of this concept for electronic beam scanning is a well-known principle for the controlled forming of radiation patterns of an active antenna element using parasitically coupled passive antenna elements.³ It allows for controlling the radiation pattern in the horizontal (azimuth) plane and steering the beam over a wide field of view. Simple electronic components such as PIN or varactor diodes may be used to tune the parasitic array elements and control beam shape and direction.

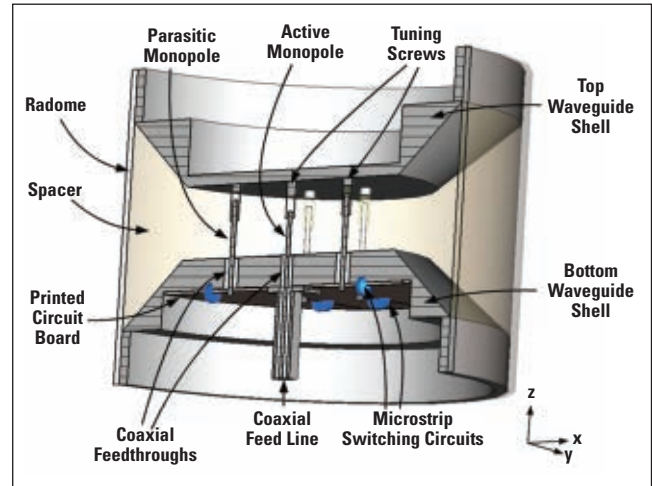
A CSPA antenna for a high-power data link application in C-Band (4.4 to 5 GHz) has been previously developed.⁴ This design uses wire monopole antennas as active and parasitic radiators, sharing a common metallic ground plane of circular shape with the active element placed at its center. These monopoles must have a height of approximately $\lambda/4$ and spacing between the active element and the parasitic elements of approximately $\lambda/4$. **Figure 5** shows a 3D model of a C-Band CSPA antenna.

For the SARABAND project, the specifications of the Q-Band CSPA antenna are shown in **Table 3**. At Q-Band the monopole-based CSPA is not feasible because of the height

of the monopoles (only 1.8 mm) and the relative size of the additional circuitry (much larger than the antenna elements). Instead, printed microstrip technology is used, based on the CSPA concept.

A demonstrator fixed-beam antenna (without switching elements) is shown in **Figure 6a**. In a forthcoming version, the beam will be steered by tuning/de-tuning the reflector elements through PIN diode biasing. Because the central active antenna element cannot achieve high gain

by itself, the radiated signal is guided through a circular flared horn. At the center frequency of 42 GHz, a standard horn structure would have a length



▲ Fig. 5 C-Band CSPA antenna 3D model.

TABLE 4

TARGET PARAMETERS FOR THE TH-RN RADIO MODULES AND ANTENNAS

Radio Module TH-RN	Parameters	Values	Variances
Receiver			
	Noise Figure	4 dB	0.5 dB over temperature range
	Saturation P_{in}	-30 dBm	
	Gain	31 dB	Temperature: ± 1.5 dB Frequency: ± 1.5 dB
Transmitter			
	P_{sat}	29 dBm	Temperature: ± 1.5 dB Frequency: ± 1.5 dB
	P_1	26 dBm	Temperature: ± 1.5 dB Frequency: ± 1.5 dB
	Gain	26 dB	Temperature: ± 1.5 dB Frequency: ± 1.5 dB

TABLE 5

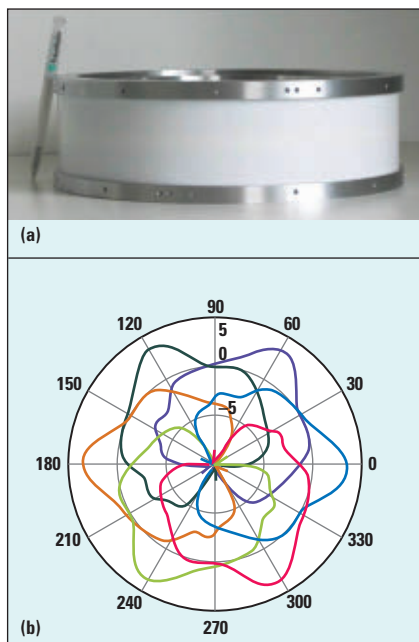
TARGET PARAMETERS FOR THE NTE RADIO MODULES AND ANTENNAS

Radio Module NTE	Parameters	Values	Variances
Receiver			
	Noise Figure	6 dB	0.5 dB over temperature range
	Saturation P_{in}	-30 dBm	
	Gain	30 dB	Temperature: ± 1.5 dB Frequency: ± 1.5 dB
Transmitter			
	P_{sat}	19 dBm	Temperature: ± 1.5 dB Frequency: ± 1.5 dB
	P_1	16 dBm	Temperature: ± 1.5 dB Frequency: ± 1.5 dB
	Gain	21 dB	Temperature: ± 1.5 dB Frequency: ± 1.5 dB

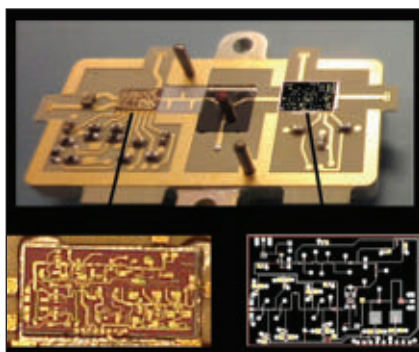
TABLE 3

CSPA ANTENNA SPECIFICATIONS

Antenna Diameter	< 300 mm
Gain	16 dBi
Polarization	Vertical
Beamwidth (E/H plane)	6°/60°
Bandwidth at -10 dB	1 GHz (41.5 to 42.5 GHz)
Ideal coverage	270° in H plane (large field of view)



▲ Fig. 6 Photograph of the fabricated fixed-beam CSPA Q-Band antenna (a) simulated radiation patterns (b).



▲ Fig. 7 NTE transceiver.

of approximately 300 mm. Due to external limitations the size of the horn must be reduced without reducing its gain; therefore, special measures are incorporated in the horn structure to reduce its size and increase the gain to achieve the desired characteristics. The antenna has an impedance bandwidth of 4.87 percent centered at 42 GHz. Simulated radiation patterns in the horizontal plane at 42 GHz are shown in **Figure 6b** for various scanning directions, corresponding to different configurations of tuned/detuned reflector elements.

RF MODULES

Front end radio modules use advanced GaAs-based monolithic microwave integrated circuit (MMIC) elements and benefit from system-in-a-package (SIP) technology integration

to reduce the printed circuit board (PCB) footprint. Specific MMIC chip-sets for the up and downconverters have been developed by the project. These integrate several different functions and provide gain improvements, achieving the 18 dBm power target for the upconverter and 31/33 dB gain for the downconverter with 2.5 dB noise factor. These two chip-sets, together with a power amplifier, are the core elements of the front end radio modules for the network nodes. **Tables 4** and **5** list target parameters for the NTE and TH-RN radio modules and antennas.

Specific SIPs using a supporting PCB etched on an organic substrate and including the MMIC chip-sets, filters, isolator/circulator and the antenna interconnection have been designed and manufactured for the SARABAND demonstrator. An example of a manufactured SIP design is the NTE transceiver shown in **Figure 7**, which consists of a 42×25 mm rectangular module. It is composed of the upconverter and downconverter chip-sets soldered on a metallic plate, and a circulator which isolates the uplink from the downlink and allows alternative transmission and reception. A specific connector adapted for 40 to 45 GHz is used for the antenna interface. Signals coming from the local oscillator and the intermediate frequency amplifier and power are supplied through the PCB. Finally, a cover plate shields the module.

One of the biggest challenges has been to successfully miniaturize the front end radio modules. The use of SIP integration and GaAs-based MMIC modules has made this possible. In addition, miniaturization has reduced circuit losses, reduced cost (low site rental, easy installation) and enhanced acceptability. In the future, novel technologies such as Si-Ge-based devices and high frequency switch components could easily be incorporated to improve the performance of the chipsets and the SIP.

CONCLUSION

The Q-Band PMP backhaul architecture developed through the SARABAND project provides multi-gigabit capacity in a cost-effective manner by exploiting PMP transmissions and the Q-Band spectrum. In addition, the

project has several on-going antenna and radio module developments. In particular, a 23 dBi gain Fabry-Perot antenna using multiple sources for medium-gain applications has been designed. Moreover, sub-wavelength structured lens antennas with gains higher than 30 dBi to cover both TH and NTE requirements have been manufactured. For electronic beam steering, a CSPA antenna has been proposed. The designed antenna has a relative impedance bandwidth of 4.87 percent, centered at 42 GHz, and a gain of 16 dBi with a beamwidth of $6^\circ/60^\circ$ (E/H plane) to cover a horizontal angular range of 270° . Finally, miniaturized front end modules with SIP integration have been designed and manufactured.

References

1. D. Jackson, P. Burghignoli, G. Lovat, F. Capolino, J. Chen, D. Wilton and A. Oliner, "The Fundamental Physics of Directive Beaming at Microwave and Optical Frequencies and the Role of Leaky Waves," *Proceedings of the IEEE*, Vol. 99, No. 10, October 2011, pp. 1780-1805.
2. A. Petosa, N. Gagnon and A. Ittipiboon, "Effects of Fresnel Lens Thickness on Aperture Efficiency," *Proceedings of the 10th International Symposium on Antenna Techniques and Applied Electromagnetics*, July 2004, pp.175-178.
3. R.F. Harrington, "Reactively Controlled Directive Arrays," *IEEE Transactions on Antennas and Propagation*, Vol. 26, No. 3, May 1978, pp. 390-395.
4. T. Bertuch, "A Circular Switched Parasitic Array Antenna for High Power Data Link Applications," *Proceedings of the 3rd European Conference on Antennas and Propagation (EuCAP)*, March 2009, pp. 2483-2487.

Ruth Vilar received her M.Sc. and Ph.D. degrees in Telecommunications from the Universitat Politècnica de València, Valencia, Spain, in 2007 and 2010, respectively. She joined the Nanophotonics Technology Center as a researcher in 2004. Her research activities are focused on backhaul and access networks, advanced optical techniques for microwave signals and ultra-high speed data transmission. Other research interests include optical performance monitoring and packet-switched networks.

Javier Martí received his Ingeniero de Telecomunicación degree from the Universidad Politècnica de Catalunya, Spain in 1991, and his Ph.D. degree from the Universidad Politècnica de Valencia, Spain in 1994. In 1989 and 1990, he was an assistant lecturer at the Universidad Politècnica de Catalunya.



From 1991 to 2000, he held the positions of lecturer and associate professor at the Telecommunication Engineering Faculty. Martí is currently the director of a national research centre for photonic technologies at the Valencia Nanophotonics Technology Centre (NTC), in Valencia, Spain. He has authored 7 patents and over 185 papers in refereed international technical journals in the fields of broadband hybrid fiber-radio systems and microwave/millimeter wave photonics, access networks, terabit/s OTDM/WDM optical networks, advanced optical processing techniques for microwave signals and ultra-high speed data transmission and silicon photonics.

Romain Czarny received his Engineering degree from ENST Paris (Ecole Nationale Supérieure des Telecommunications, now Télécom ParisTech) in 2002. He joined Thales Research & Technology (TRT) in 2006 where he received a Ph.D. in collaboration with IEMN working on optically driven sub-millimeter sources. After three years as project manager in a Thales subsidiary, Czarny joined the TRT LCDT Laboratory (Component, Technologies Integration & Demonstration Lab) with activities dedicated to optical concepts applied to RF technologies such as millimeter wave imaging and lens antenna technologies.

Maciej Sypek received his M.Sc., Ph.D. and habilitation degrees from the Warsaw University of Technology in 1987, 1992 and 2009, respectively. He is now the CEO of the Polish innovative company Ortech, active in the areas of information technologies and optics. He deals with optical design and numerical simulations of propagation electromagnetic radiation in demanding configurations from the extreme ultra-violet to the terahertz range. Sypek is an expert in the design and characterization of sub-wavelength elements. He is an author and co-author of more than 50 articles published in pre-reviewed scientific journals.

Michał Makowski received his M.Sc. and Ph.D. degrees from the Warsaw University of Technology in 2001 and 2007, respectively. His activities in Ortech are focused on the fabrication and characterization of sophisticated, optical, diffractive and holographic elements for the wide range of frequencies. Makowski is an author and co-author of more than 40 articles published in pre-reviewed scientific journals.

Cédric Martel joined the antenna department of ERA Technology (UK) in 1997. In 2002, he received his Ph.D. degree following a part-time research

program in collaboration with ERA Technology and the University of Surrey. Since January 2006, he has been working as an antenna research engineer in the department of electromagnetism and radar (DEMR) of ONERA in France. Martel's research interests include leaky wave antennas, reconfigurable antennas, phased arrays, metamaterials and their antenna applications.

Thomas Crépin received his M.S. degree in physics from University of Lille, France, in 2002 and his Ph.D. degree from the University of Lille, France, in 2006. From 2002 to 2006, he was with Institut d'Electronique, de Microélectronique et de Nanotechnologie (IEMN), Lille, France, where he worked on terahertz technology and metamaterials. Crépin is currently working in the field of antenna and metamaterial design at ONERA, The French Aerospace Lab, in the Electromagnetism and Radar Department, Toulouse, France.

Fabrice Boust received the Agrégation of Physics in 1981 from the École Normale Supérieure de l'Enseignement Technique. He earned a Doctorate of Science in 1989 from the Paris Sud University. Boust is currently a senior expert in the Radar Department of ONERA (the French Aerospace Lab) and in SONDRRA (a joint laboratory established between Supélec, ONERA, the National University of Singapore and DSO National Laboratories). His research interests are dynamics of magnetic particles, radar absorbing materials and metamaterials for antennas.

Ronald Joseph received his Ph.D. degree from Kumamoto University, Japan in 2011. He was a Lecturer in Electronics at Christ Junior College, Bangalore, India from 2002 to 2008. Joseph is currently working at the Fraunhofer Institute for High Frequency Physics and Radar Technique, FHR, Wachtberg, Germany. His research interests are antenna design and electromagnetic modeling.

Kai Herbertz received his Ph.D. in electrical and electronic engineering from Imperial College London, U.K., in 2010. Since 2011, Herbertz has been working as a researcher for the Fraunhofer Institute for High Frequency Physics and Radar Techniques (Fraunhofer FHR). His research interests include metamaterials and electromagnetic modeling.

Thomas Bertuch received his Ph.D. from RWTH Aachen University, Aachen, Germany, in 2003. His doctoral research

was developed at the Research Institute for High Frequency Physics and Radar Techniques of the Research Establishment for Applied Natural Science e.V. (FGAN-FHR), Wachtberg, Germany. In 2004, he was a senior antenna scientist with the Defence, Security and Safety Institute of The Netherlands Organization for Applied Scientific Research (TNO), The Hague, The Netherlands. Since 2005, Bertuch has been with the FGAN-FHR which, since 2009, is the Fraunhofer Institute for High Frequency Physics and Radar Techniques (Fraunhofer FHR); where he is currently Team Leader of Antennas and Front End Technology. From 2000 to 2009, he was Lecturer of RF engineering at the Bonn-Rhine-Sieg University of Applied Sciences, Sankt Augustin, Germany. Since 2012 he has been Lecturer of Antennas and Wave Propagation at the Aachen University of Applied Sciences, Aachen, Germany. Bertuch's research activities include antenna and microwave circuit design, engineered electromagnetic materials (metamaterials), radar system design and electromagnetic modeling.

Alain LeFevre graduated from the Conservatoire des Arts et Métiers specializing in Macromolecule Polymers. He joined the Thales microwave department in 2000 to develop microwave component industrial activities and became involved in IFF (Identification Friend or Foe) microwave and X-Band activities. He has been in charge of studying a Q-Band Solid State Power Amplifier in the Thales microwave department.

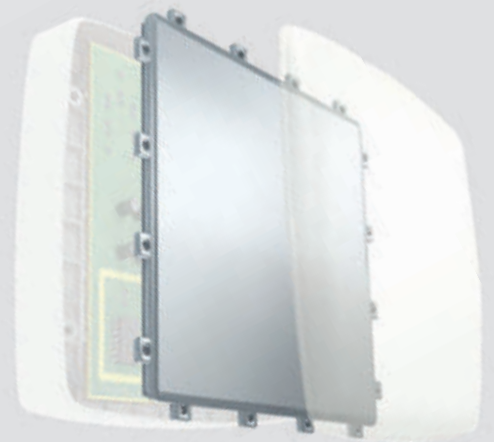
François Magne is responsible for research and development at Bluwan. He began his career at the French DGA (French department of defence), creating missile guidance and directional radar systems. He later became director of industrial relations at French research think tank CNRS, and went on to lead advanced research at TRT-Philips and Thomson CSF. When the Thales Group acquired Thomson CSF, he became the chief scientist for the Thales CNI (communication, navigation and identification) division. Magne was a critical contributor in the development of advanced communications systems, as well as the development of satellite and high speed broadband technologies. In 2002, he became the vice president of technology in charge of innovation and industrialization at Thales, with whom he co-founded Bluwan in 2005.



SENCITY®Matrix flat antenna

Low visual impact – high data-traffic

- Ideal antenna for 60 and 70/80 GHz
- Lowest weight, smallest size
- Great TCO, competitive pricing
- Replace bulky dish antennas
- Integrates easily into street level environment
- Allows fast installation



Disruptive Factors in the Global Long Haul Market

Emmy Johnson
Sky Light Research, Scottsdale, Ariz.

Last summer, Sky Light Research (SLR) published a special report on the long haul market for North America. Due to LTE and its IP data centric requirements, long haul radios in North America were undergoing a transformation – becoming much more compact, flexible, powerful and fast. As of summer 2013, these slimmer, more agile radios were only available for the North American market, however, as SLR predicted, these radios are now available for the global market. Over the last year and a half, several vendors have add-

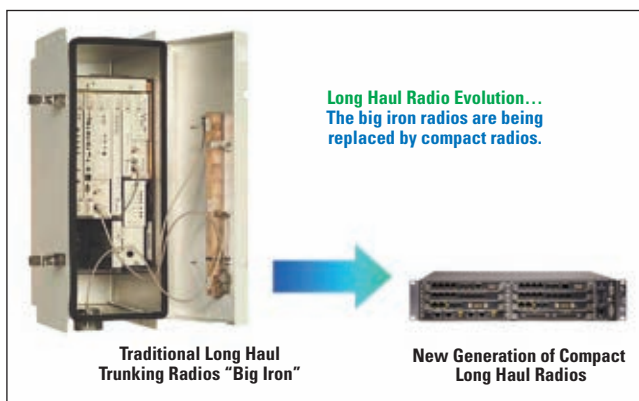
ed new or improved long haul product offerings to their portfolios.

This new concept of IP based long haul radios has created two categories: (1) traditional big iron long haul radios, often referred to as trunk radios, and (2) new compact IP based long haul radios (see **Figure 1**). Although the requirement for the traditional “big iron”, high power trunking radios exists, Sky Light Research believes that growth in the long haul segment will be driven by the new IP based long haul radios.

CHANGING SPECIFICATIONS

The difference between the two types of long haul radios is illustrated in **Table 1**. Often companies offer both types, with traditional radios appealing legacy customers and projects, while compact IP based long haul radios attract customers modernizing their networks with IP. The changing specifications that are highlighted in Table 1 include:

Agile Architecture: Many vendors offering traditional trunking radios have updated their products to have a split mount version, since many operators cannot afford or do not want the expense associated with the shelters and required air conditioning needed to support a traditional microwave trunking solution. By placing part of the radio outside, it



▲ Fig. 1 Long haul radio evolution.

TABLE I

CHANGING SPECIFICATIONS

	<i>Traditional Trunking/ Long Haul Radios</i>	<i>New IP Based Long Haul Radios</i>
Architecture	Full Indoor	Split-Mount/All Outdoor/ All Indoor
Capacity	4 to 6 Gbps per Antenna	up to 16 Gbps per Antenna
Carriers	8 to 12	10 to 20
Transmission Protocol	TDM Based	IP Based/Hybrid
System Gain	< 100 dB with waveguide	> 100 dB with waveguide
Transmission Power (dBm)	25 to 30	30 to 35
OAM	SDH based	Ethernet Service Capable (IEEE 1588v2, Ipv6)
Power Consumption	100+ W per channel	Under 100 W per channel

reduces the footprint and the expense required to keep the shelter and the equipment cool.

Traditional long haul or trunking radios are “big iron” radios that have large footprints. In some cases, especially in the non-mobile verticals, these radios are still preferred. However, mobile operators are driving the growth in the long haul segment, and they require a different type of architecture to resolve the quandary of limited real estate that is becoming increasingly expensive. This is one of the driving changes for long haul radios. Newer, compact IP-based long haul radios can now be used outdoors, indoors or in a split mount configuration.

All outdoor radios can be hung on poles, eliminating the footprint in the cabinet. This architectural change has expanded the use of long haul not only to the core, where a cabinet exists, but also to the cell's edge, due to its smaller form factor.

With its MPR9500 MPT-HL for the North American market, Alcatel Lucent was first-to-market with this concept. Until 12 to 18 months ago, Alcatel-Lucent owned the IP based compact long haul market in North America. Other vendors quickly realized the market potential and developed their own radios. Operators now have several options for compact IP based long haul solutions as LTE rolls out across the globe.

Capacity: It is well known that capacity requirements in the network

antenna, making it one of the highest capacity radios on the market.

Power: Like capacity, power also is increasing. The defining characteristic for long haul or trunking radios is high power, which makes them able to send the signal a longer distance (hence the name long haul). Today, long haul radios are pushing the power threshold, reaching 35 dBm, which emasculates the traditional 20 to 26 dBm of a few years ago. SIAE's radio can reach 35 dBm with 20 dB automatic transmit power control (ATPC).

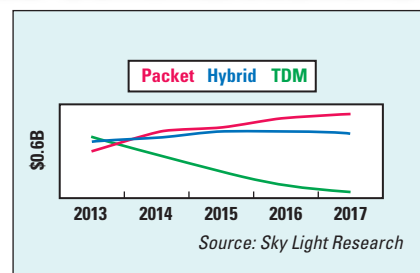
Hybrid/IP based: Long haul radios with TDM are still required in many cases, due to TDM's ability to handle issues such as multi-path fading. However, future growth in long haul radios will be driven by Hybrid and/or IP based radios. This movement is making hybrid radios a more strategic choice over TDM radios for those customers who need a smooth transition from TDM to IP. Trunking/long haul radios are often used at aggregation points or in the backbone of the network where various types of media come together. Hybrid radios, by definition, can natively service the various traffic types, making them an important piece in the microwave tool kit. IP based long haul radios, however, are ideal for mobile data networks, like LTE and HSPA, where increased capacity is a must in order to support more IP packet-based services and applications.

Green/Energy Efficient: As with all networking infrastructure equip-

are on an upward trajectory. Long haul radios approach capacity slightly differently than short haul radios. The unique characteristic of long haul radios is its branching mechanism. This allows the aggregation of several carriers on one antenna, which creates a very high capacity radio.

For example, Huawei's new long haul IP based radio is able to reach 16 Gbps – by aggregating 16 carriers of 1

Gbps each to one



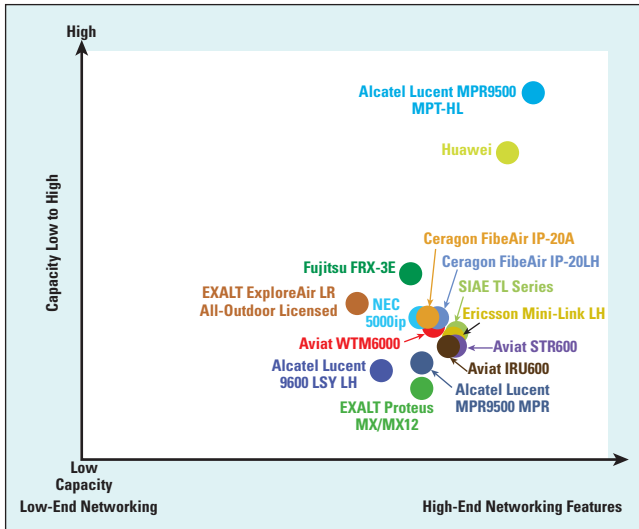
▲ Fig. 2 Global long haul forecast.

ment, energy efficiency is important. Whether the trunk radio is being used in a fixed line provider's central office located in a remote region, or it's being hung on a pole in a mobile operator's network in a suburb, going green is important. Previously, radios were using over 100 W per channel; however, long haul radios today use less. Aviat's STR-600 long haul radio is one of the most efficient on the market, using less than 60 W per channel.

SLR expects 2014 to be the first year where we see IP based long haul radios out-ship TDM radios (see **Figure 2**). This has already occurred in North America since the North American market is the region where long haul has the greatest demand. The shift in North America was driven by mobile operators rolling out LTE. Historically, mobile operators played a small part in long haul revenue generation due to their reliance on short haul radios. One of the central changes in the new long haul radios is its flexible architecture/compact footprint that is similar to short haul radios. Equipment vendors are taking full advantage of this feature, appealing to operators' desire to save real estate.

For example, both Ceragon's and Aviat's IP based long haul radios are available in split-mount. This architectural option has some resemblance to short haul radios that operators are used to deploying and building into their networks. Several vendors now selling compact IP based long haul radios will have a positive effect on growth for long haul radios through the forecast period.

Although compact IP based long haul revenue outside of North America is still in its infancy, SLR believes that this will change in the next 12 to 18 months, with strong growth occurring worldwide. There are just a handful of equipment manufacturers who offer compact IP based long haul radios for regions outside of North



▲ Fig. 3 Networking features – low end to high end.

America, with Alcatel-Lucent and Huawei being among them. These two vendors represent a market bell-wether of sorts because:

- 1) Alcatel-Lucent is the first to have compact IP based long haul radios, and they have had great success in the North American market. Even though most of the demand stemmed from just two customers, AT&T and Verizon, the company clearly sees the benefit that compact IP based long haul radios offers a mobile operator deploying advanced mobile broadband services.
- 2) Huawei is a leading microwave vendor and has never had a long haul offering. Since they are making their foray into the long haul market with an IP based compact long haul radio, they must have some very large customers asking for this solution. Huawei has been aggressive in winning 4G bids and SLR suspects that this latest radio is a product driven from customer requests.

THE LONG AND THE SHORT OF THE LONG HAUL MARKET

Historically, global long haul revenue has paled in comparison to short haul revenue. Despite this, long haul radios are a vital and steady market for the manufacturers that sell them worldwide. Although they are not used as much as short haul radios, their price points are much higher, with prices typically between \$14,000 and \$40,000 a link, depending on the application and load. The higher price

Private networks use long haul to connect remote locations to a headquarters for redundant links or for public safety, security and surveillance. Mobile operators use them nearer the central office to transport the traffic generated from cell sites on the edge back to the core. Public and private networks use long haul for connecting metro or building rings in the core of the network when fiber is not a practical solution. Because of their mission critical applications, long haul radios need to be highly reliable with high capacity data services. To achieve the multi gigabit capacity often required, most long haul radios support technologies like XPIC.

COMPETITIVE LANDSCAPE

The competitive landscape for long haul/trunk radios is dominated by less than a dozen equipment vendors. All of these, except Fujitsu, have a traditional short haul microwave radio offering as well. Some of these vendors are new to the long haul market, and are using their strong position in the short haul arena to leverage long haul sales.

Alcatel-Lucent: Alcatel-Lucent was the first to have a compact IP based long haul radio. Their innovative 9500 MPR platform has been tried and tested in real LTE deployments and thus, Alcatel-Lucent understands what mobile operators require for mobile broadband long haul deployments. The MPR 9500 long haul version offers 20 channels/antenna, up to 16 Gbps, and carrier class Ethernet services like redundancy, IEEE 1588 v2 and Synch E.

points, combined with new applications for IP based compact long haul, will rejuvenate the market and drive up revenue.

Long haul radio applications run the gamut from backhaul to interconnecting buildings. Key verticals include utility companies, government agencies, enterprises, public service agencies, fixed line service providers and mobile operators.

Aviat: Aviat has three long haul/trunking solutions – WTM6000, STR600 and IRU600, with the IRU600 only for North America. The WTM6000 is a traditional trunking radio, while the STR600 is split-mount. The trunking radio can support up to 16 channels, transport 4 Gbps of traffic and has a L2 carrier Ethernet switch. The STR600 does not require waveguides which makes the radio much more economical and provides better system performance than higher power all indoor trunking radios.

Ceragon: Ceragon's long-haul portfolio is built around the new, SDN-ready IP-20 platform and comes with a range of ANSI and ETSI configurations. Ceragon's fully protected longhaul solutions feature high density and high capacity and offer rich functionality. The IP-20 Platform simplifies the migration from Native TDM and Hybrid to all packet architectures. Because the new IDUs are completely backwards compatible with Ceragon's entire portfolio, including FibeAir and Evolution radio units, Ceragon customers require the replacement of only the IDU while keeping the radios, antennas, branching and waveguides/coax intact.

Ericsson: Ericsson has long been the leading microwave vendor and one of the leading vendors in the trunking/long haul radio market. They have recently made some changes to the Mini-Link LH radio, by offering a flexible, semi-compact or trunking version. The Mini-Link LH is part of its Mini-Link platform, offering interchangeable short haul and long haul radios for maximum flexibility and scaling.

Fujitsu: Fujitsu has one of the most OEM'd trunking/long haul radios around. Several microwave radio vendors private label their FRX-3E. Fujitsu prides itself on offering true hybrid quality. So instead of being solely focused on Ethernet services, and possibly sacrificing some traditional features, such as N+1 SDH, that can be critical for multi-path fading, Fujitsu is focused on helping customers facilitate a smooth migration from TDM to Ethernet.

Huawei: Huawei has been a leading vendor in the short haul market and has recently introduced a com-

pact IP based radio for the long haul market. Their radio seems to have all the bells and whistles – compact, very high capacity (16 Gbps), up to 16 channels, up to 34 dBm transmit power and all the required Ethernet services.

NEC: NEC has two long haul radios – the 5000S (TDM) and the more recently introduced 5000IP (Hybrid/IP). Both radios are indoor, “big iron” radios. The 5000IP has ethernet OAM for fault management and performance monitoring as well as multiple clock sources such as synchronous Ethernet, IEEE 1588v2 and legacy TDM synchronization.

SIAE: SIAE’s TL trunking radio is a hybrid radio that offers 16 channels per rack. It not only supports variable bandwidth options, but also supports Ethernet services such as Synch E and IEEE 1588 v2. Its very high power of 35 dBm is one of the highest available.

The features listed above are all important, but how do equipment vendors stack up on the key specifications? SLR surveyed radio vendors based on the metrics listed in Table 1 and then assigned a score to each. These were then tabulated for a networking score (see **Figure 3**) – the higher the aggregated score, the further to the right of the chart the radio lies. The higher the capacity, the further to the top of the chart the radio lies.

Specifications were from vendors’ data sheets and claims they made on surveys. Some of these claims were not able to be verified. If no information could be found, assumptions were made. ■



Emmy Johnson is the founder and principal analyst of Sky Light Research, a third-party analyst firm specializing in wireless point-to-point mobile backhaul technologies such as microwave, sub 6 GHz and millimeter wave radios. The firm’s popular services include

quarterly market share reports and forecasts. Sky Light Research was founded in 2001 and is located in Scottsdale, Ariz. For more information, please email info@SkyLightResearch.com or call (480) 563-2251.



2015

Electronic Design Innovation Conference

电子设计创新会议

Connecting Engineers and Industry

April 14-16, 2015

Beijing, China

北京

CALL FOR PAPERS

In April 2015, the leading technical conference and exhibition developed by and for the RF, microwave, EMC/EMI and high speed electronics industry returns to Beijing. Share your expertise with fellow technologists as a speaker in the EDI CON technical program.

Technical papers accepted for EDI CON will adhere to *Microwave Journal* standards of excellence through a similar peer review process, providing conference delegates with high-quality, unbiased, practical technical content.

Topics

- Design
- Measurement & Modeling
- Systems Engineering
- Commercial Applications

Submit your paper online

For details go to:

www.ediconchina.com/CallForPapers.asp

Deadline: November 30, 2014

Exhibition Spaces Available

www.EDICONCHINA.com



Locating Sources of Interference

Cyril Noger, Anritsu S.A.
Villebon-sur-Yvette, France

The proliferation of RF devices has benefited the world in many ways, providing readier and more convenient access to communications, entertainment and information. But it has come with one unintended drawback: a huge increase in the frequency and severity of incidents of interference.

Cellular telephone networks have been hit particularly hard: the introduction of many new cellular technologies to an ever-growing number of subscribers has made it difficult for the network operators and spectrum regulation authorities to find clean spectrum unaffected by interference. Interference in cellular transmissions increases noise, with the effect of:

- reducing the effective size of a cell
- lowering data rates delivered to user equipment
- impairing the quality of voice and data communications

As a result, radio technicians spend much time travelling around the country, hunting the sources of interference. Only once a source is precisely located can action be taken to lower the power of its transmissions or to disable it entirely, if appropriate.

On occasion, filtering an unwanted in-band signal can solve the problem. Otherwise, the technician's job is to monitor the spectrum, uncover the nature of an interferer (permanent or intermittent) and track it to its source.

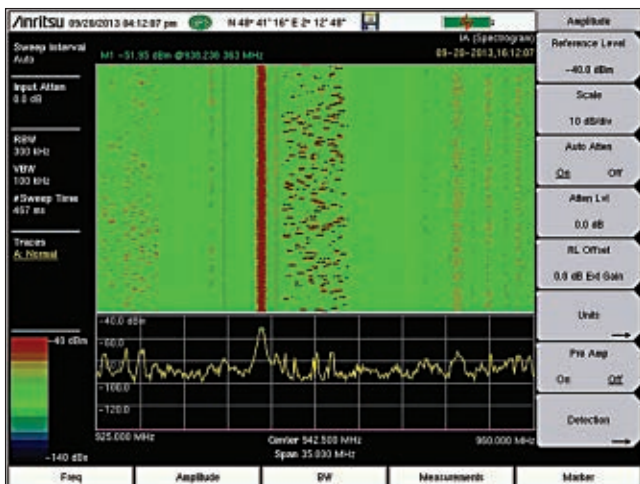
TYPES OF INTERFERENCE AFFECTING CELLULAR NETWORKS

The existence of interference affecting a cell is normally obvious to the operator, because it

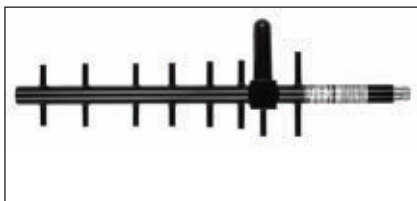
will have caused a drop in communications performance which will have been reported by the operator's networking monitoring systems. The first step in dealing with the problem is to observe what is happening in the affected frequency band. At this stage, the technician needs to know whether the interference is continuous or intermittent by measuring the amplitude and power of the interfering signal(s). This is best done by connecting an omnidirectional antenna to a spectrum analyzer, placing it in the cell in question and leaving it to log network activity for a period of time.

The analyzer may find one or more of a number of types of interference:

- In-band interference: an unwanted signal from a different transmitter type that falls inside the operating bandwidth of the desired signal. This corrupts the receiver as it is difficult to filter.
- Co-channel interference: similar to in-band interference, except that the unwanted signal originates from a transmitter in the same network, but located elsewhere.
- Out of band interference: in a wireless system designed to transmit in a different frequency band, part of a transmitted signal's energy can fall into the operating frequency band of the cell under test, impairing its performance.
- Adjacent channel interference: often seen in wideband transmission systems, when transmissions at the main operating frequency also generate lower-amplitude signals in directly neighboring channels (called the lower and upper channels or left and right channels).



▲ Fig. 1 Spectrogram showing occurrences of signals in the GSM frequency band over a period of a few minutes.



▲ Fig. 2 A Yagi antenna can isolate an interference source at a particular frequency.



▲ Fig. 3 A Log Periodic antenna can capture a variety of interferers across a wide frequency spectrum.

- Uplink and downlink interference: unwanted signals affecting the receiver (uplink) or the transmitter (downlink) of a base station when it communicates with a mobile terminal.
- Impulse noise: created whenever a flow of electricity is abruptly started or stopped, impulse noise can affect any transmitter's or receiver's characteristics, with the effect of scrambling communications.

Other types of interference may be found, but the most common types are those listed.

LOCATING THE SOURCE

In today's cellular telephone networks, the operator will be alerted to a problem by built-in alarms or dedicated sensors distributed through the

network which can time-stamp instances of interference. Now, radio technicians have to identify the cause of the problem.

If the source of the problem is an RF emitter, one way to troubleshoot the system is to monitor the frequency band of the affected transmitter or receiver. A modern handheld spectrum analyzer connected to an omnidirectional antenna can accurately monitor a frequency band over a period of time (typically up to 72 hours) by continuously logging spectrum measurements.

Figure 1 shows the spectrogram display of continuous measurements. Its advantage is that the power (amplitude) of each detected frequency is color-coded, so when analyzing the measurements it is easy to see whether or not an unwanted signal appears in the frequency band under investigation. This first step will commonly identify the frequency and amplitude of the interfering signal, and the nature of its emissions (random, regular or continuous). Measurements taken from a single location are not sufficient to precisely locate the interferer.

The next step is to attempt to locate the source with the use of directional antennas (see **Figures 2** and **3**). In the past, the preferred way to locate a source was to use an analog meter to measure the strength of a signal or carrier (see **Figure 4**). These meters gave an audible beep which rose in frequency as the signal strength rose. This allowed technicians driving vehicles with roof-mounted antennas to gauge signal strength without taking their eyes off the road. While this was convenient, it was not an accurate means to locate interference, as the meter had no embedded mapping capability.

An improvement on this method is to perform a mapped drive test. Using the same omnidirectional antenna mounted on the roof of a car, the technician drives on a route through the affected area logging the power of signals at the suspected frequency. By

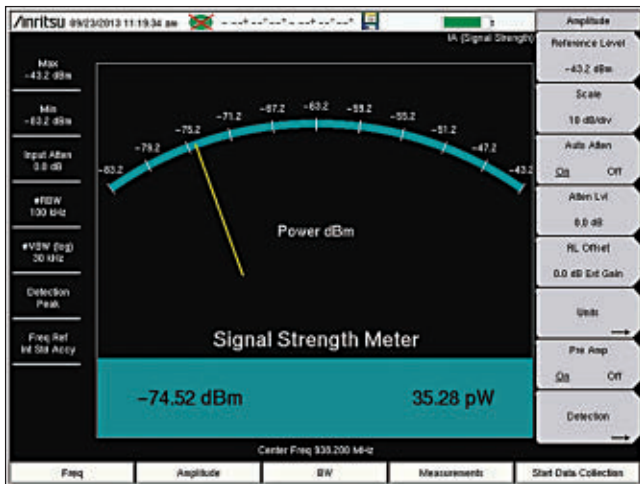
IDA 2: Dive Deep into Interference Analysis



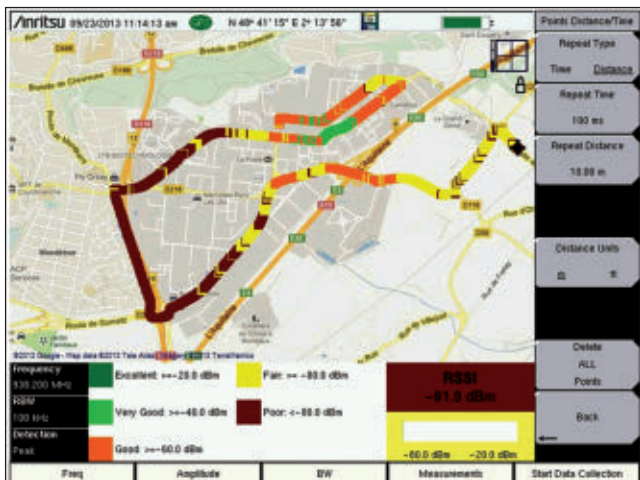
Rapidly identify, precisely analyze, easily evaluate and intelligently localize interference in the radio spectrum.

- Extremely fast: 12 GHz/s
- Super light: < 3 kg
- Impressively sensitive: NF 7 dB
- I/Q-Analyzer: Real-time in-field analysis
 - 1 μ s spectrogram resolution
 - Persistence display

Narda Safety Test Solutions GmbH
Sandwiesenstrasse 7
72793 Pfullingen, Germany
Tel. +49 7121 97 32 0
info.narda-de@L-3com.com
www.narda-ida.com



▲ Fig. 4 A spectrum analyzer can emulate the display style of an analog meter to show signal strength.



▲ Fig. 5 A drive test records the signal strength at a chosen frequency over the course of a known route.



▲ Fig. 6 Direction finding in the field with a handheld spectrum analyzer and unidirectional antenna.

pre-loading the route into a software application such as easyMap Tools, a map can be hosted on the spectrum analyzer and directly displayed while driving. As **Figure 5** shows, the analyzer can display the car's location in real-time (derived from a GPS signal) and the power of the received signal at the chosen frequency (known as Received



▲ Fig. 7 Triangulation locates the source of interference on the instrument's map.

Signal Strength Indicator, or RSSI).

The easyMap Tools software allows for the car's variable speed: the user can configure the spectrum analyzer to take a measurement at set distances, for example, every 10 m. Subsequent analysis of the drive test results might indicate the area in which the interfering signal is strongest.

To this point the interference-hunting process has narrowed

the search down to a small area. But it has not precisely located the source: this means that the technician can still not identify it, so it cannot be attenuated, filtered or disabled. Finding the precise location of the interferer calls for the use of the same handheld spectrum analyzer, but now with a directional, narrowband antenna. The process of 'direction finding' in the suspected area is uncovered by the drive test.

Since this normally involves going out on foot in the area under investigation while holding a portable spectrum analyzer, it is helpful to have an accessory for holding the directional antenna. For example, Anritsu provides the MA2700A, an ergonomic handle that secures the antenna via a standard connector (see **Figure 6**).

The MA2700A also includes a broadband pre-amplifier to boost the antenna's sensitivity and a built-in

GPS receiver to enable the precise location at which measurements are taken to be logged in the spectrum analyzer. Finally, a built-in electronic compass (magnetometer) senses the exact direction in which the antenna is pointed. The user just has to pull a trigger and turn around 360° to find the direction of the strongest signal at the frequency in question. The location and direction are displayed on the instrument's screen.

By repeating this process from multiple locations, the user can perform triangulation (see **Figure 7**); the various measurements should almost always point towards a single location on the map. This is the source of the interference.

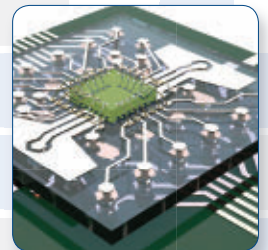
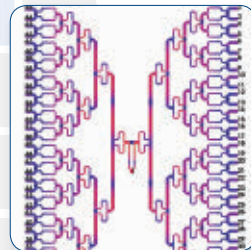
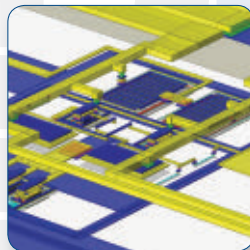
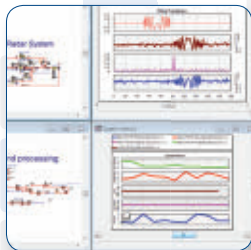
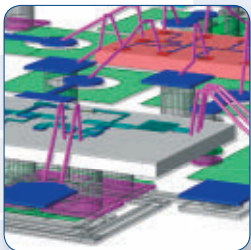
This technique can be used by any network technician, since it uses familiar equipment and easy-to-operate software tools. Normally, this technique on its own is sufficient to enable the technician to find and fix the interference problem.

There are many kinds of interference sources that affect the performance of wireless transmission systems. The handheld spectrum analyzer, combined with omni- and unidirectional antennas, is the most convenient and effective instrument for identifying and locating the position of the interferer. In addition, by integrating GPS and mapping software in the spectrum analyzer, the time taken to troubleshoot interference problems is minimized.

VENDORVIEW

Anritsu S.A.
Villebon-sur-Yvette, France
www.anritsu.com

Try NI AWR Design Environment Today!



Microwave Office | Visual System Simulator | Analog Office | AXIEM | Analyst

Try NI AWR Design Environment

today and see for yourself how easy and effective it is to streamline your design process, improve end product performance, and accelerate time to market for MMICs, RFICs, RF PCBs, microwave modules, 3D/planar passive interconnects, antennas, communication systems, and more.

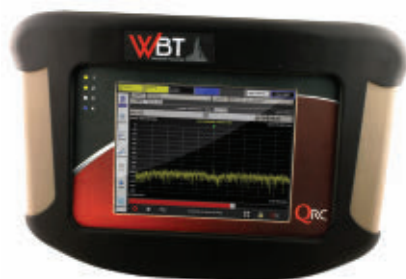
>> Learn more at ni.com/awr

NI AWR Design Environment consists of a comprehensive software product portfolio that offers a variety of high-frequency design tools that embrace system simulation, circuit simulation, and electromagnetic analysis.

- Microwave Office for MMIC, module, and RF PCB design
- Visual System Simulator for RF/comms. systems design
- Analog Office for analog and RFIC design
- AXIEM for 3D planar electromagnetic analysis
- Analyst for 3D FEM EM simulation and analysis



Visit awrcorp.com/whatsnew for a complete list of features found in the current version of NI AWR Design Environment.



Transcorder Records 80 MHz Bandwidth Between 50 MHz and 6 GHz

QRC Technologies
Fredericksburg, Va.

The WBT-200 Wideband Transcorder® by QRC Technologies records and plays back 80 MHz of RF bandwidth, in two separately tunable 40 MHz sections, anywhere between 50 MHz and 6 GHz.

Contained in a single box and weighing less than 10 lbs, the WBT-200 is capable of playing back the recorded signals anywhere within the tuning range without the need for any additional equipment (see **Figure 1**). It eliminates

the need for a separate spectrum analyzer to digitize the signal, a signal generator to play back the RF and a PC to interface and control the unit. The WBT-200's simple user interface has a single button for RF record or playback.

Many other RF recording and playback systems require additional equipment with numerous interconnects, which increases the total cost of ownership and complicates the test setup and run procedures for the user. According to QRC Technologies, the WBT-200 has better performance and costs less than other similar products, most of which only collect data and can't reconstruct and play back the RF.

WBT APPLICATIONS

The WBT-200 can be used for the following applications:

Reference Signal Recording and Playback: A reference signal (e.g., test cases, standard compliance vectors) can be recorded, easily recalled and repeatedly played back. The WBT can replace expensive single-purpose communication test sets, which is especially advantageous in manufacturing operations that require numerous workstations to certify products.

Signal Analysis: Analysis can occur while the signal is being recorded, either by playing the recording back or directly analyzing the data.



▲ Fig. 1 WBT-200 display showing RF playback.



▲ Fig. 2 RF spectrogram obtained with the spectrum waterfall app.

Market Penetration: Utilization of licensed spectrum can be measured easily and quickly.

Competitive Analysis: A rough comparison of mobile operators can be obtained by measuring the amount of licensed spectrum each utilizes.

Interference Analysis: Looking directly at the spectrum can often determine the presence of an unlicensed signal. Playing back the recording can prove this to the interfering entity.

Training: The RF environment of interest can be recorded and played back to personnel being trained.

Receiver Test and Design: Particular signal configurations and tests can be recorded and played back for a deterministic design and test of RF receivers.

Security: The presence of unwanted transmissions can be detected anywhere in the frequency range.

Arbitrary Waveform Transmitter: Programmatically generated waveforms (e.g., in MATLAB) can be easily transmitted.

In the near future, the WBT-200 will also simultaneously record and retransmit 40 MHz of received spectrum in realtime at a different center frequency, enabling it to be used as a repeater or downconverter.

DATA STORAGE AND TRANSFER

The WBT platform records to and plays back from standard 2.5" commercial solid state drives (SSD) using the VITA 49 Radio Transport (VRT) industry standard open format. SSDs have the necessary read and write speeds and ensure a robust, portable

product that will withstand shock and vibration.

The WBT-200 includes two drive bays. While data is recorded and played back using one SSD, the other SSD can easily be replaced without affecting the operation of the system. This unlimited disk swapping enables continuous recording and playback, limited only by the number of SSDs available.

Data on the drives can be visualized and analyzed using the WBT's Signal Analysis Toolkit or other analysis packages that utilize the QVRT file format.

If the signal has less than 80 MHz of instantaneous RF bandwidth, the recording bandwidth can be reduced to conserve disk space.

A gigabit Ethernet port is provided to transfer data from the SSDs over a network, remotely control a WBT and allow one WBT to control other WBTs. A future capability will allow data to be streamed directly to another device, at greatly reduced bandwidth. The interface supports both DHCP and static network configuration.

An eSATAp (powered eSATA) port enables additional high-speed disks to be directly connected to the WBT. In the future, data may be recorded directly onto the eSATA disks; however, maximum bandwidth may be reduced, depending on disk performance.

TIMING AND SYNCHRONIZATION

The WBT-200 contains an embedded GPS disciplined oscillator (GPS-DO) that provides a precise internal 10 MHz timing reference, which is made available externally. The oscillator also generates a 1 pulse per second (PPS) signal with ± 50 nanosecond accuracy, also available externally. These frequency and timing reference ports can be used to synchronize the WBT with other components, including additional WBTs for simultaneous recording and playback.

The 50-channel GPS receiver has an acquisition sensitivity of -144 dBm

and tracking sensitivity of -160 dBm. The RF recordings are tagged with GPS geo-location.

WBT APPS

To expand the utility of the WBT-200, QRC has created a series of applications that supplement the role of many test systems. A patented, open architecture application programmer's interface (API) and VRT-based IQ file format (QVRT) make it possible. The WBT's core firmware provides the basic hardware level control of the system and application management. Everything else is available through the WBT API and open for anyone to use.

The following free apps will soon be available to download and install from the online WBT App Store:

Spectrum Waterfall: RF spectrogram (see *Figure 2*).

AGC: Configurable automatic gain control of both WBT receivers.

SCPI Control: WBT control via Standard Commands for Programmable Instruments.

Timed Record/Playback: Record and/or playback files at specified times.

Tune and Dwell: Record specific sections of spectrum for a specific time and loop, if necessary.

Level Trigger: Record when power exceeds a threshold (peak or average), for a user-defined time, and stop recording when the signal falls back below a user-set power threshold.

RF DVR: In a temporary buffer, perpetually store the last received RF data for a user-defined duration. When a user-defined event has occurred, users can write the buffered RF information to the disk and continue to record the RF following the event.

Sweep To File: Sweep from a start to a stop frequency and save the spectrum results as a CSV file for analysis.

Users can also develop custom applications — even resell them through the WBT App Store — using common tools and languages such as C++, Python and familiar programming environments like Qt. QRC offers a full, prepackaged development environment and all necessary documentation.

QRC Technologies
Fredericksburg, Va.
(540) 446-2270
<http://wbt.qrctech.com/>



Field Analyzer with PIM Testing Capability

duct PIM versus time, swept PIM, distance-to-PIM (DTP), return loss, VSWR, cable loss and distance-to-fault (DTF) measurements. In addition to eliminating the need to carry multiple instruments to the top of a tower, the integrated MW82119B PIM Master allows all site data to be stored in one location for fast retrieval.

The MW82119B PIM is MIL-STD-810G drop test rated and is designed to withstand transportation shock, vibration and harsh outdoor test conditions. The MW82119B PIM Master has also achieved an IP54 ingress protection rating, certifying its ability to operate without damage after exposure to blowing dust and water spray.

The MW82119B PIM Master has an outdoor viewable 8.4" display and intuitive user interface (UI) that is op-

timized for field conditions. New stainless steel lifting rings in the chassis and a padded soft case make the analyzer well suited for hoisting during tower-top testing. The analyzer's rugged design, lightweight and small size enable both PIM and line sweep testing at the top of the tower.

Covering various bands and featuring unprecedented measurement capability, the MW82119B PIM Master is well suited for a number of applications, including the deployment and maintenance of LTE remote radio heads (RRH), small cells and distributed antenna systems (DAS).



Anritsu Co.
Morgan Hill, Calif.
www.anritsu.com

Anritsu Co. has introduced the MW82119B PIM Master™ that combines a 40 W, battery-operated PIM analyzer with a 2 MHz to 3 GHz cable and antenna analyzer, eliminating the need to carry multiple instruments to measure the RF performance of a cell site. The MW82119B provides tower and maintenance contractors, network installers and wireless service providers with the first handheld field passive intermodulation (PIM) analyzer with line sweep capability that fully certifies cell site cable and antenna systems.

The MW82119B PIM Master with Site Master™ option supports the full array of site tests. Field users can con-



Low PIM, Plenum Rated Cable Assembly and mini-DIN Connector

The Times SPP-LLPL 50 ohm, low loss plenum rated/UL listed coaxial cable assembly family has been expanded to include SPP-375-LLPL 3/8" and SPP-500-LLPL 1/2" cables for even lower loss. With excellent electrical performance compared to many other copper cable assemblies, SPP-LLPL cables are well suited for in-building solutions for PIM-sensitive installations and system interconnects. Meeting the fire resistance requirements of UL 910 for plenum rated applications, the new larger sizes of SPP-LLPL cable assemblies are ideal for installations where lower loss is needed. High quality connectors assure excellent and reliable static and dynamic PIM performance: better than -155 dBc for

applications up to 6 GHz. All Times plenum cables are UL listed and printed with the UL file number. SPP-LLPL cable assemblies are available in 1, 2 and 3 meter pre-assembled lengths with N, 716 DIN and SMA connector interfaces, and the new 4.1/9.5 mini DIN connectors.

The new 4.1/9.5 mini-DIN straight male connector, TC-SPP250-4195M-LP, is available for the SPP-250-LLPL (SuperFlexible Plenum PIM) 50 ohm low loss plenum rated coaxial cable assemblies for use in distributed antenna system (DAS) applications. SPP-250-LLPL is a 1/4" super flexible type corrugated cable with low den-

sity PTFE dielectric and FEP jacket that meets the requirements of UL 910 for plenum applications. The cable assemblies are suitable for in-building jumpers and interconnects up to 6 GHz. The factory installable connectors attach via soldering of the center pin and induction soldering to the cable outer conductor, providing excellent VSWR performance and reliable PIM performance better than -155 dBc.

Times Microwave Systems
Wallingford, Conn.
(203) 949-8400
www.timesmicrowave.com

SPINNER || MOBILE COMMUNICATION



SPINNER is a global leader in developing and manufacturing state-of-the-art RF components. Since 1946, the industries leading companies have trusted SPINNER to provide them with innovative products and outstanding customised solutions.

Headquartered in Munich, and with production facilities in Germany, Hungary and China the SPINNER Group has over 1.100 employees worldwide.

Our subsidiaries and representatives are present in over 40 countries and provide our customers with an international network of support.

SPINNER GmbH || Germany
info@spinner-group.com
www.spinner-group.com



Getting started with 4.3-10

Our 4.3-10 portfolio is consistently growing. Now available:

- Calibration Kits and EasyDock for Test & Measurement
- Connectors, Adaptors and Jumpers
- Loads and Attenuators
- Couplers and Splitters

... more to come



High Frequency Performance Worldwide



DC to 6 GHz SDR

Crimson is a flexible, wide-band, high gain Software Defined Radio (SDR) platform that comes equipped with four independent receive and four independent transmit chains, each capable of up to 322 MHz of RF bandwidth to 6 GHz. At the core of the digital front, Crimson is powered by an Altera™ Arria V FPGA (5ASTMD3E3F31I3N) with an on-chip, dual-core ARM Cortex-A9 processor, and comes with a high stability internal reference clock.

Crimson has an RF tuning range of

100 kHz to 6 GHz with receive gain of 67 dB, SFDR of 55 dB at 200 MHz, SNR up to 73 dB and P1dB of -11 dBm. The transmit power is 10 dBm maximum at 6 GHz with P1dB of 14 dBm and SFDR of 61 dB from DC to 500 MHz.

Features

- Operating frequency from DC to 6 GHz (MF-HF-VHF-UF)
- Over 1200 MHz of RF bandwidth across four independent, controllable Rx channels, and over 1200 MHz across four independent, controllable Tx channels
- Low noise and high dynamic range
- High stability internal reference clock (± 5 ppb)

- On-board Altera ST FPGA with ARM processor
- Dual 10 Gigabit Ethernet back-haul

Applications

- Near real-time signals analysis
- Signal recording and spectrum monitoring
- Spectrum allocation analysis
- Multiple-input-multiple-output (MIMO) applications
- Mobile backhaul and base station
- Wideband communications

Per Vices

Toronto, Canada

solutions@pervices.com

www.pervices.com



Frequency Matters.

Go *Mobile*

with the MWJ APP

Get the free Microwave Journal Magazine App that includes the monthly issue, favorite archives and real-time industry news, blogs and interviews. Available on iTunes, Google Play and Amazon.

Download Now



<http://bit.ly/VQxL2o>

Download your MWJ app now
at www.mwjjournal.com/MWJapp



COMPANY SHOWCASE



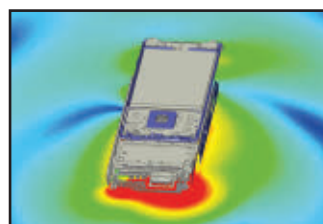
RF and Microwave Technology



Anaren Inc. is a Syracuse-based, global leader in RF and microwave technology used in wireless infrastructure, satellite, defense and consumer-electronics applications. The company has approximately 1,000 employees and five state-of-the-art facilities worldwide. Product lines include: standard passive components (e.g., couplers, power dividers, baluns, resistors, attenuators, terminations), RF multichip modules, high-reliability softboard and ceramic PCBs, and complex assemblies (e.g., switching, beamformers, antenna feed networks, DRFMs, IMAs).

Anaren Inc.

www.anaren.com



EM Simulation for Mobile Communications



As mobile communication devices become thinner, smaller and more complex with every generation, designs need to meet new standards of performance. Using electromagnetic (EM) simulation,

engineers can not only design and optimize the antenna of mobile devices, but also test its performance within the handset, for example, by evaluating coupling effects and the impact of dielectric materials, and investigating the influence of the human body on performance. Find out more about CST STUDIO SUITE®, an EM simulation tool, by visiting the company's website.

Computer Simulation Technology AG (CST)

www.cst.com



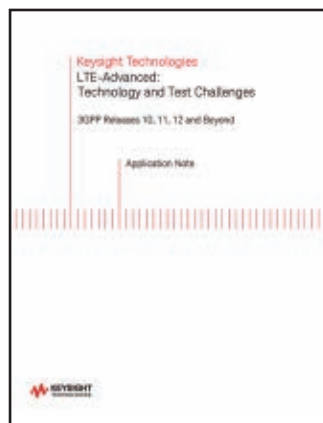
Flat Antennas SENCITY Matrix

As mobile data traffic levels continue to rise, small cells are increasingly being seen as a vital component of a modern heterogeneous network. The small size of HUBER+SUHNER SENCITY® Matrix antennas allows operators to access rooftop, wall and street level sites. HUBER+SUHNER offers a range of stand-alone antennas including radome, back-plane and standard waveguide-

interface that allows for quick adaption of this revolutionary technology. For entirely individual radio designs the antennas can also be purchased without housing. Visit www.hubersuhner.com for more information.

HUBER+SUHNER

www.hubersuhner.com



LTE-Advanced Application Note



Keysight Technologies' LTE-Advanced: Technology and Test Challenges application note offers insights into 3GPP Releases 10, 11, 12 and beyond, with a focus on the LTE-Advanced air interface. It also covers 3GPP specifications for core network standards and services. Topics include LTE and LTE-Advanced, including summaries of LTE Release 8/9 features, ITU requirements for 4G, and 3GPP requirements for LTE evolution; Release 10 and LTE-Advanced;

Release 11 LTE-Advanced enhancements; Release 12 radio evolution; Release 13 update; and LTE-Advanced product design and testing challenges.

Keysight Technologies Inc.

www.keysight.com



Equipment & Components Catalog



Celebrating its 53rd anniversary, MECA (Microwave Equipment & Components of America) designs and manufactures an array of Low PIM DAS Equipment and RF/microwave components with industry leading performance. MECA is recognized worldwide as a primary source of supply for rugged and reliable components to commercial and military OEMs, service providers and installers by only providing products made in the U.S. Download the company's

components catalog at www.e-meca.com/pdfs/MECA_catalogo-2014.pdf.

MECA Electronics Inc.

www.e-MECA.com



Custom Rack Mount Test Equipment Guide



Mini-Circuits announced the publication of the 2014 Custom Rack Mount Test Equipment Guide, a 52-page, full color brochure showcasing a wide selection of custom test solutions ranging from DC to 18 GHz including amplifiers, signal generators, routing and distribution systems, and more. The brochure highlights Mini-Circuits' ability to deliver affordable, reliable custom test solutions with turnaround times as fast as two weeks and also introduces the

company's user-friendly control software, programming support and test accessories. To request a copy, email sales@minicircuits.com.

Mini-Circuits

www.minicircuits.com



COMPANY SHOWCASE



Advancing the Wireless Revolution

VENDORVIEW

NI AWR software products accelerate the design and product development cycle of high-frequency ICs and systems found within the aerospace/defense, semiconductor, computer, consumer electronics and telecommunications markets by reducing the time it takes from concept through manufacturing. NI AWR Design Environment provides an intuitive use model that delivers an exceptional user experience and open design flow that

supports third party tools, resulting in more compelling solutions. These unique aspects of NI AWR software maximizes user productivity by eliminating errors and design redundancies, quickening the pace to market.

National Instruments (formerly AWR Corp.)

www.ni.com/awr



Filters, Multiplexers and Multifunction Assemblies

VENDORVIEW

Reactel offers a variety of filters, multiplexers and multifunction assemblies for the mobile communication industry. Reactel's experienced engineers can come up with a creative solution for all of your Tx, Rx or co-site requirements. Reactel has designed a broad range of filters from high power units operating to 5 kW and beyond to extremely small ceramic units that are suitable for handheld or portable applications. The company's product line includes bandpass, lowpass, highpass and notch filters as well as multiplexers and multi-passband filters. Offering fast turnaround, competitive pricing and high quality, Reactel can satisfy most any requirement you may have.

Reactel Inc.

www.reactel.com



T&M Instruments That Meet Your Needs

VENDORVIEW

Whatever your job is, you do not always need the ultimate high-end T&M equipment. You do need precise, reliable, universal measuring instruments. That is what you get with Value Instruments from Rohde & Schwarz. They combine practical features with excellent measurement characteristics that are easy to use and easy on the budget. Find out more in the Value Instruments Catalog 2014 from Rohde & Schwarz. (Order number: PD 3606.6463.42).

Rohde & Schwarz GmbH & Co. KG

www.rohde-schwarz.com



Getting Started With 4.3-10

SPINNER GmbH released their new 4.3-10 catalog. The catalog reflects the current 4.3-10 products showing connectors, jumpers, measurement and calibration, loads and attenuators, and couplers and splitters. The SPINNER Group has been setting standards with its RF technology products for more than 65 years. The company's high quality standards for design, material and manufacturing ensure the best possible connectivity, optimized installation and failure-free operation, even under the toughest environmental conditions. For more information visit the company's website at www.spinner-group.com.

Spinner GmbH

www.spinner-group.com

ADVERTISING INDEX & SALES REPRESENTATIVES

ADVERTISER	PAGE NO.
Anaren Microwave	31
CST of America, Inc.	17
EDI CON 2015	39
Huber + Suhner AG	35
Keysight Technologies	COV 4
MECA Electronics, Inc.	9
Microwave Journal	48
Mini-Circuits	13, 21
Narda Safety Test Solution GmbH	41
National Instruments	43
Reactel, Incorporated	27
Rohde & Schwarz GmbH	COV 3
Skyworks Solutions, Inc.	COV 2
Spinner GmbH	47
Ed Kiessling, Traffic Manager/Inside Sales 685 Canton Street Norwood, MA 02062 Tel: (781) 619-1963 FAX: (781) 769-6178 ekiessling@mwjournal.com	

Eastern and Central Time Zones
Chuck Boyd
Northeast Reg. Sales Mgr.
(New England, New York, Eastern Canada)
685 Canton Street
Norwood, MA 02062
Tel: (781) 769-9750
FAX: (781) 769-5037
cboyd@mwjournal.com

Michael Hallman
Eastern Reg. Sales Mgr.
(Mid-Atlantic, Southeast, Midwest)
4 Valley View Court
Middletown, MD 21769
Tel: (301) 371-8830
FAX: (301) 371-8832
mhallman@mwjournal.com

Pacific and Mountain Time Zones
Brian Landy
Western Reg. Sales Mgr.
(CA, AZ, OR, WA, ID, NV, UT, NM, CO, WY, MT, ND, SD, NE & Western Canada)
144 Segre Place
Santa Cruz, CA 95060
Tel: (831) 426-4143
FAX: (831) 515-5444
blandy@mwjournal.com

International Sales
Richard Vaughan
International Sales Manager
16 Sussex Street
London SW1V 4RW, England
Tel: +44 207 596 8742
FAX: +44 207 596 8749
rvaughan@horizonhouse.co.uk

Germany, Austria, and Switzerland
(German-speaking)
WMS.Werbe- und Media Service
Brigitte Beranek
Gerhart-Hauptmann-Street 33,
D-72574 Bad Urach
Germany
Tel: +49 7125 407 31 18
FAX: +49 7125 407 31 08
bberanek@horizonhouse.com

Israel
Liat Heblum
Oreet International Media
15 Kineret Street
51201 Bene-Berak, Israel
Tel: +972 3 570 6527
FAX: +972 3 570 6526
liat@oreet-marcom.com

Korea
Young-Seoh Chinn
JES Media International
2nd Floor, ANA Bldg.
257-1, Myungil-Dong
Kangdong-Gu
Seoul, 134-070 Korea
Tel: +82 2 481-3411
FAX: +82 2 481-3414
yschinn@horizonhouse.com

Japan
Katsuhiko Ishii
Ace Media Service Inc.
12-6, 4-Chome,
Nishiiku, Adachi-Ku
Tokyo 121-0824, Japan
Tel: +81 3 5691 3335
FAX: +81 3 5691 3336
amskatsu@dream.com

China
Michael Tsui
ACT International
Tel: 86-755-25988571
Tel: 86-21-62511200
FAX: 86-10-58607751
michaelt@actintl.com.hk

Hong Kong
Mark Mak
ACT International
Tel: 852-28366298
markm@actintl.com.hk

Dreamteam for success.

Please visit us at the
Mobile World Congress
in Barcelona,
hall 6, booth C40

Signal generation and analysis for demanding requirements

When working at the cutting edge of technology, you shouldn't waste your time with inferior tools. Rely on measuring instruments evolved in the spirit of innovation and based on industry-leading expertise. Instruments like the R&S®SMW200A vector signal generator and the R&S®FSW signal and spectrum analyzer. Each is at the crest of today's possibilities. As a team, they open up new horizons.

See for yourself at www.rohde-schwarz.com/ad/highend



ROHDE & SCHWARZ

We know LTE-Advanced.

In fact, our engineers co-wrote the book on it.

We know what it takes for your designs to meet LTE-A standards. After all, Keysight engineers have played significant roles in LTE-A and other wireless standards bodies and forums, including 3GPP. Our engineers even co-authored the first book about LTE-A design and test. In addition, we have hundreds of application engineers. You'll find them all over the world, and their expertise is yours for the asking.

HARDWARE + SOFTWARE + PEOPLE = LTE-A INSIGHTS

Representative on every key wireless standards organization globally

Hundreds of applications engineers in 100 countries around the world

Thousands of patents issued in Keysight's history

Download a free chapter of the *LTE and the Evolution to 4G Wireless* book at www.keysight.com/find/LTE-A-Insight

USA: 800 829 4444
CAN: 877 894 4414



Unlocking Measurement Insights